Gas phase ion-ion recombination and electron capture reactions at atmospheric pressure
by John Allen Culbertson

A thesis submitted in partial fulfillment of the requirements for the degree of Doctor of Philosophy in Chemistry
Montana State University

Abstract:
Gas phase ion processes at high pressure (one atmosphere) are the basis of some of the most sensitive and selective analytical techniques for chemical analysis, ie. the electron capture detector (BCD), the atmospheric pressure ionization mass spectrometer (APIMS) , and the ion mobility spectrometer. Under most conditions, ion-ion recombination (IIR) will be the dominant loss mechanism for ions in high pressure ionized gases. Therefore, it is of fundamental importance to understand IIR. In this thesis work, relative IIR rate constants were determined using an APIMS. Also, a new method was developed for the determination of the fate of molecular anions upon recombination with positive ions at atmospheric pressure. These results were used to predict the atmospheric chemistry of certain perfluorocompounds (PFC's). This method also proved to be effective for determining the electron capture (EC) rate constants of compounds that undergo dissociative EC.

The APIMS showed that for all ions studied, the IIR rate constant was the same, approximately 2 x 10^-6 cm^3 sec^-1. The experimental apparatus developed for the determination of the fate of molecular anion upon IIR allowed for the comparison of two BCD responses for the compound being studied. The first was a normal BCD response. The second BCD response was obtained after the gas chromatographic carrier gas was passed through a reaction cell in which EC and IIR reactions occurred. The ratio of these two responses was interpreted in terms of the extent to which the molecule was lost to EC and then regenerated by IIR. The conclusions were that the molecular anions of C7F14 (perfluoromethylcyclohexane) and C6F12 (perfluorodimethylcyclobutane) regenerate their parent neutrals upon IIR while the molecular anion of SF6 does not. The molecular anions of nitrobenzene and several substituted nitrobenzenes were also studied and showed varying extents of regeneration. The same experimental procedure was also used to determine EC rate constants for compounds that could not be regenerated by IIR.

GAS PHASE ION-ION RECOMBINATION AND ELECTRON CAPTURE REACTIONS AT ATMOSPHERIC PRESSURE

by

John Allen Culbertson

A thesis submitted in partial fulfillment
of the requirements for the degree

of

Doctor of Philosophy

in

Chemistry

MONTANA STATE UNIVERSITY
Bozeman, Montana

October 1995

APPROVAL

of a thesis submitted by

John Allen Culbertson

This thesis has been read by each member of the thesis committee and has been found to be satisfactory regarding content, English usage, format, citations, bibliographic style, and consistency, and is ready for submission to the College of Graduate Studies.

10/30/95
Date

Chairperson, Graduate Committee

Approved for the Major Department

10/30/95
Date

Head, Major Department

Approved for the College of Graduate Studies

12/14/95
Date

Graduate Dean

STATEMENT OF PERMISSION TO USE

In presenting this thesis in partial fulfillment of the requirements for a doctoral degree at Montana State University, I agree that the Library shall make it available to borrowers under rules of the Library. I further agree that copying of this thesis is allowable only for scholarly purposes, consistent with "fair use" as prescribed in the U.S. Copyright Law. Requests for extensive copying or reproduction of this thesis should be referred to University Microfilms International, 300 North Zeeb Road, Ann Arbor, Michigan 48106, to whom I have granted "the exclusive right to reproduce and distribute my dissertation in and from microfilm along with the non-exclusive right to reproduce and distribute my abstract in any format in whole or in part."

Signature 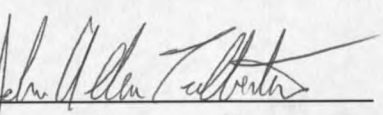

Date 10-30-95

TABLE OF CONTENTS

TABLE OF CONTENTS-Continued

LIST OF TABLES

LIST OF FIGURES

LIST OF FIGURES-Continued

ABSTRACT

Gas phase ion processes at high pressure (one atmosphere) are the basis of some of the most sensitive and selective analytical techniques for chemical analysis, ie. the electron capture detector (ECD), the atmospheric pressure ionization mass spectrometer (APIMS), and the ion mobility spectrometer. Under most conditions, ion-ion recombination (IIR) will be the dominant loss mechanism for ions in high pressure ionized gases. Therefore, it is of fundamental importance to understand IIR. In this thesis work, relative IIR rate constants were determined using an APIMS. Also, a new method was developed for the determination of the fate of molecular anions upon recombination with positive ions at atmospheric pressure. These results were used to predict the atmospheric chemistry of certain perfluorocompounds (PFC's). This method also proved to be effective for determining the electron capture (EC) rate constants of compounds that undergo dissociative EC.

The APIMS showed that for all ions studied, the IIR rate constant was the same, approximately 2×10^{-6} cm^3 sec^{-1}. The experimental apparatus developed for the determination of the fate of molecular anion upon IIR allowed for the comparison of two ECD responses for the compound being studied. The first was a normal ECD response. The second ECD response was obtained after the gas chromatographic carrier gas was passed through a reaction cell in which EC and IIR reactions occurred. The ratio of these two responses was interpreted in terms of the extent to which the molecule was lost to EC and then regenerated by IIR. The conclusions were that the molecular anions of C_7F_{14} (perfluoromethylcyclohexane) and C_6F_{12} (perfluorodimethylcyclobutane) regenerate their parent neutrals upon IIR while the molecular anion of SF_6 does not. The molecular anions of nitrobenzene and several substituted nitrobenzenes were also studied and showed varying extents of regeneration. The same experimental procedure was also used to determine EC rate constants for compounds that could not be regenerated by IIR.

INTRODUCTION

Gas Phase Ion Chemistry

During the past 25 years, gas phase ion chemistry (GPIC) has been a steadily growing research field (1),(2),(3). This is due in part to the fact that the intrinsic properties of ions and molecules are best studied in the gas phase, where solvent effects can be eliminated or carefully controlled. Also, some of the most selective and sensitive analytical techniques for chemical analysis are based upon GPIC. Such techniques include ion cyclotron resonance (ICR) mass spectrometry (MS) (4), chemical ionization (CI) MS (5), electron capture detection (ECD) (6), atmospheric pressure ionization (API) MS (7), ion mobility spectrometry (IMS) (8), and electrospray MS (9). These techniques operate over a wide pressure range, from 10^{-5}-10^{-6} Torr for ICR, to 0.1 - 0.5 Torr for CIMS, to atmospheric pressure for ECD, APIMS, IMS, and electrospray MS. In spite of this wide pressure range, most of the instrumentation used to study the fundamentals of GPIC operate at less than 10 Torr. Such instruments typically employ a mass spectrometer to select and measure the ions of

interest. These MS-based instruments include ICR, flowing afterglow (10), selected ion flow tube (10), and pulsed electron high pressure MS (11), all of which have contributed significantly to the wealth of valuable GPIC information that exists at lower pressures. In contrast, studies of GPIC at pressures greater than 10 Torr are very few, due mainly to the lack of capable instrumentation in the past. However, there is a clear need to understand high pressure GPIC processes in order to increase the performance of analytical instruments that operate at or near atmospheric pressure (such as the ones listed above), thoroughly interpret the results obtained from such instruments, or to design new high pressure instrumentation. In addition, gas phase processes at low pressure are often significantly different from those at high pressure. Thus, predictions of GPIC at high pressure based on low pressure results often fail. This basic lack of knowledge of high pressure gas phase processes was the motivation for this thesis work. Two processes in particular, ion-ion recombination (IIR) and electron capture (EC), are the focus of this work and are discussed below.

Electron Capture

Several of the most selective and sensitive techniques for chemical analysis are based on the electron capture process. The most widely used of these, and the one used for a great deal of this thesis work, is the electron capture detector. The first description of the ECD was by Lovelock (12) in 1960. While the modern ECD is quite different from the first ones described by Lovelock, the fundamental characteristics are similar.

The ECD is very selective in that only molecules with positive electron affinities and sufficiently large electron capture cross sections are detected, which comprise a small minority of compounds. A molecule meeting these criteria may attach a low energy electron to form a molecular anion (resonance capture) or a fragment anion (dissociative capture) The mechanism of the electron capture process is discussed in the Theory section.

The ECD response is based on changes in the electron population within the detector. In most ECD's, electrons are collected at an anode that is pulsed at approximately +50 volts. The resulting current is then measured and maintained

at some fixed value by adjusting the pulse frequency, thus the term, constant current ECD is used. When a compound that attaches electrons enters the detector, the electron population decreases, causing an increase in the pulse frequency. The response at the chart recorder is proportional to the change in pulse frequency. In other ECD's, such as the dual cell ECD used in this work, the anode is pulsed at a fixed frequency. Thus, a change in electron population results in a change in the current measured at the anode. This type of ECD is well suited for fundamental studies in that the dynamics of the ECD can be changed by adjusting the pulse frequency and/or pulse width.

Ion-Ion Recombination

The dominant loss mechanism for ions in most high pressure ionized gases is ion-ion recombination. Diffusion of ions to grounded surfaces or removal by carrier gas flow is typically much slower than IIR (13). For this reason, IIR is a very important reaction within the ECD, and the products of the IIR reaction may influence the ECD response to certain compounds.

Consider the following reaction sequence which can occur

within the ECD.

$$M + e \rightarrow M^- \quad (1)$$

$$M^- + P^+ \rightarrow M + \text{neutrals} \quad (2a)$$

$$M^- + P^+ \rightarrow Z + \text{neutrals} \quad (2b)$$

Reaction 1 is resonance electron capture by which the molecular anion, M^-, is formed. Reactions 2a/b represent the two possible pathways of the subsequent IIR between the molecular anion and positive ions. In reaction 2a, IIR results in the regeneration of the parent molecule, M, while in reaction 2b the parent molecular entity has been altered upon IIR. If the parent molecule is regenerated, it may undergo additional EC/IIR reactions. This will result in an enhanced response to that compound relative to the case in which altered neutrals are formed upon IIR (Reaction 2b). This type of behavior can give anomalous responses in gas phase coulometry (14) experiments and may also have important implications to the atmospheric chemistry of perfluorinated compounds (15), which is discussed below.

Atmospheric Fates of Perfluoro Compounds

Fully fluorinated compounds (perfluoro compounds or PFC's) represent a class of chemicals which include many

species that exhibit extreme inertness to chemical and photochemical reactions. This results in most PFC's being immune to the processes that typically remove trace chemicals from the atmosphere, ie., photodissociation and reaction with radicals (15). Therefore, PFC's may be transported through the troposphere (the first 15 km of the atmosphere) and stratosphere (15 to 50 km), to the mesosphere (50 to 90 km). Only in the mesosphere are important destructive processes for PFC's thought to exist. These destructive processes include absorption of Lyman-α radiation (121.6 nm) and reaction with free electrons. The latter means of destruction can potentially be more important than photolytic destruction for those PFC's that have relatively large EC rate constants. These EC active compounds are known to include SF_6 (16), c-C_4F_8 (15), and larger cyclic carbon based PFC's, such as C_7F_{14} (perfluoromethylcyclohexane) (17), and $C_{10}F_{18}$ (perfluorodecaline) (18). Furthermore, it is known that these molecules capture thermalized electrons primarily by the resonance EC process (Reaction 1) in which the molecular anion is formed. Therefore, in determining the atmospheric chemistry of these EC active PFC's, the critical question is: what will be the neutral products formed in the subsequent recombination

of these molecular anions with positive ions, as represented in Reactions 2a/b. If the original molecule is simply regenerated in these IIR reactions, as in pathway 2a, the sequential EC/IIR reactions will have no impact on the overall atmospheric chemistry of that compound. If, on the other hand, the molecular entity is altered by the IIR reaction, as shown in pathway 2b, the atmospheric presence of that compound will be terminated by its EC reaction.

Because PFC's are not believed to destroy stratospheric ozone, they were considered environmentally friendly, and some were thus suggested as replacements for the ozone depleting chlorofluoro compounds (15). However, PFC's are expected to have extraordinarily long atmospheric lifetimes (on the order of millennia) due to their chemical and photolytic inertness, and thus significant global warming potentials (GWP) (15). The GWP is a measure of the relative efficiency of a gas to contribute to global warming (the greenhouse effect) by absorption of infrared radiation, per kilogram emitted (15). Therefore, even if relatively small amounts of PFC's are emitted into the Earth's atmosphere, they would accumulate over time and their impact could be very significant in future years.

Morris et al.(15) have predicted that for some PFC's which attach electrons rapidly, the EC/IIR process could account for at least 90% of their removal in the mesosphere if the molecule is, in fact, destroyed by its sequence of EC and IIR reactions. Based on this fact, it is clear that the need to know whether or not a PFC is regenerated upon IIR, as in Reaction 2a, is of central importance. Therefore, this thesis will focus on the fractional regeneration of several PFC's upon IIR at near atmospheric pressure. Work was also performed to determine what effects the nature of the recombining ions has on the rate constant for IIR. The same experimental apparatus used for determining the fractional regeneration of PFC's was also proven to be a very effective method for determining EC rate constants for dissociatively attaching compounds. EC rate constant for many such compounds were determined for the first time in an atmospheric pressure buffer gas.

THEORY

Chemistry and Dynamics Within the Reaction Cell/ECD

As was mentioned in the Introduction, the chemistry and dynamics of gas phase processes at or near atmospheric pressure are quite different from those at low pressure. Therefore, in order to characterize the reaction cell/ECD apparatus, these processes must be understood.

The increased gas density at atmospheric pressure results in a shorter mean free path and therefore a greater collision frequency, f, between molecules. This is the fundamental difference between the high and low pressure regimes. A value for f can be obtained at any given pressure by Equation 3,

$$f = \bar{v}\sigma\sqrt{2}\frac{N}{V} \qquad (3)$$

where $\bar{v}$ is the relative mean velocity of the molecule, σ is the collision cross section, and N/V is the gas number density. A value for σ can be obtained from $\sigma=\pi d^2$ where d is the collision diameter of the molecule (19). For N_2 (d =

3.7×10^{-10}m) (19) at 640 Torr and 120°C, $f = 5.2 \times 10^{9}$ sec $^{-1}$. However, in the low pressure regime where techniques such as PHPMS and ICR are often employed to study GPIC, collision frequencies are much smaller. For example, in an ICR cell operating at 10^{-5} torr, f is approximately 100 sec^{-1}.

The high collision frequency at atmospheric pressure serves to stabilize any excited ions or molecules that are within the cell and quickly bring them to thermal equilibrium with the buffer gas. This is important because species with excess internal energy are often formed from the ionization process or other energetic reactions. Under most experimental conditions encountered at atmospheric pressure, any excited species will be thermalized in 10 collisions and a Maxwell-Boltzmann energy distribution will be achieved in about 100 collisions with the buffer gas (20).

All chemistry occurring in the reaction cell is initiated by Reaction 4, in which a beta particle, β, from a ^{63}Ni foil

$$\text{Buffer gas} + \beta \rightarrow P^{+} + e \qquad (4)$$

collides with a buffer gas molecule to produce a positive ion, P^{+}, and a secondary electron. The average kinetic energy of the beta particle is 17 keV (13) and approximately 35 eV is required to produce one P^{+}/e pair (21), therefore, 458 P^{+}/e

pairs are formed per beta. The secondary electrons are thermalized by subsequent collisions with the buffer gas. The rate of change in positive ion or electron concentration in the cell with no sample present is given by Equation 5 (22),

$$\frac{dn_e}{dt} = \frac{dn_+}{dt} = \frac{S}{V} - Rn_e n_+ \qquad (5)$$

where n_e and n_+ are the electron and positive ion densities respectively, S is the production rate of electrons governed by the activity of the ^{63}Ni foil, R is the positive ion-electron recombination rate constant, and V is the volume of the cell. Applying the steady state assumption to Equation 5, the equilibrium concentration for n_e and n_+ can be calculated from Equation 6.

$$n_e = n_+ = \sqrt{\frac{S}{VR}} \qquad (6)$$

With a volume of 1.5 cm^3, R given as 3 x 10^{-6} cm^3 sec^{-1} (23), and a 13 mCi foil (4.8 x 10^8 disint sec^{-1}), the electron density is calculated to be 1.4 x 10^{8} cm^{-3}. For all experiments in which the reaction cell was used, the electron density in the cell was determined experimentally using a reference compound whose electron capture rate constant is well known. This procedure will be discussed in detail in the

Results and Discussion section.

The thermalized electrons can interact with species present in the cell via Reactions 7-9.

$$e + P^+ \rightarrow \text{neutrals} \quad (7)$$

$$e + MX \rightarrow MX^- \quad (8)$$

$$e + MX \rightarrow M + X^- \quad (9)$$

Positive ion-electron recombination , Reaction 7, was discussed above in describing electron and ion densities. Reactions 8 and 9 are resonance and dissociative electron capture, respectively. Resonance EC results in a molecular anion, while a fragment atomic anion is produced from dissociative EC. Electron capture will occur when a molecule with a sufficiently large electron attachment cross section enters the cell. An excited intermediate negative ion, MX^{-*}, is initially formed upon EC. The reaction will proceed to completion forming a stable anion only if MX^{-*} is sufficiently long lived so that either the excess internal energy can be quenched through collisions to form a thermalized molecular anion or bond rupture can occur to produce a fragment anion.

The negative ions within the cell will be destroyed by ion-ion recombination, shown in reactions 2a/b. IIR will be discussed in detail in the following section. Two other

possible loss mechanisms for negative ions are ventilation out of the cell via carrier gas flow and diffusion to the wall of the cell resulting in charge neutralization. Both are considered negligible for the reasons described below.

Ventilation

The first order rate constant for ventilation, k_v, is given by Equation 10, where F is the flow rate of the carrier

$$k_v = F/V \tag{10}$$

gas in $cm^3\ sec^{-1}$ and V is the volume of the cell. With a typical flow rate of 0.34 $cm^3\ sec^{-1}$ and a cell volume of 1.5 cm^3, $k_v = 0.22\ sec^{-1}$. The rate of loss due to IIR, is given by Equation 11.

$$Rate_{IIR} = -k_{IIR}\ [P^+]\ [N^-] \tag{11}$$

The concentrations of positive and negative ions are given by $[P^+]$ and $[N^-]$ respectively. Under the experimental conditions used here, the positive ion concentration is in large excess and constant, thus, pseudo first order kinetics apply and Equation 11 can be rewritten as follows:

$$Rate_{IIR} = -k'_{IIR}\ [N^-] \tag{12}$$

where $k_{obs} = k_{IIR} [P^+]$. Using a k_{IIR} value of 2×10^{-6} cm^3 sec^{-1} (24) and $[P^+]$ of 1.2×10^7 cm^{-3}, determined from Equation 6, $k'_{IIR} = 24$ sec^{-1}. As can be seen, k_{obs} for IIR is approximately two orders of magnitude larger than k_v, hence ventilation is not considered important loss mechanism relative to recombination.

Diffusion

At charge densities of approximately 10^7 cm^{-3} and above, the interaction between positive and negative charge clouds becomes sufficiently strong that the gas must be treated as a plasma, with local charge neutrality being the rule (13). Any deviation from charge neutrality induces electric fields that oppose the charge separation and tend to restore charge balance. Because the diffusion of electrons is approximately 1000 times faster than that of positive ions, there is a space charge potential that develops as the electrons attempt to diffuse to areas of lower concentration, the grounded surface of the cell wall in this case. An area of negative charge develops near the cell wall, while an area of positive charge develops in the interior of the cell volume. These space charges greatly restrain the motion of electrons towards the cell wall but have the opposite effect on the positive ions,

causing them to diffuse at about twice as fast as they would in the absence of electrons (25). Consequently, the electrons and positive ions diffuse at the same velocity and can be characterized by a single ambipolar diffusion coefficient.

The charge density in the reaction cell used in this work was typically on the order of 1×10^7 cm^{-3}, therefore ambipolar diffusion conditions were operative. When an EC active compound was introduced into the cell, its concentration was kept sufficiently low so that electrons were in large excess of the negative ions produced from EC. Under these conditions, diffusion of negative ions to the wall of the cell is probably prohibited by the space charge described in the proceeding paragraph. Thus, diffusional loss of negative ions can most likely be discounted. However, if the negative ions do diffuse to the walls as rapidly as the positive ions and electrons, the first order rate constant for that process will be given by $k_d = D_a/\Lambda^2$ (25), where D_a is the ambipolar diffusion coefficient ($D_a = 2D$, where D is the free diffusion coefficient for the ion) for the ions and electrons and Λ is the characteristic diffusion length of the ion source (25). The free diffusion coefficient can be calculated (26) using the general expression $D = 3.33 \times 10^{-3}\ T^2/P(\alpha M_r)^{1/2}$, where T is

temperature (°K), P is pressure (Torr), α is the polarizibility of the buffer gas molecule (Å^3), and M_r is the reduced mass of the ion and buffer gas. For an ion of 100 amu in nitrogen at 393 K and 640 Torr (α for N_2 = 1.73 Å (19)), a value for D_a of 0.24 cm^2 sec^{-1} is obtained. Λ may be calculated by dividing the radius of the cell (0.4 cm) by π to give 0.13 cm. Therefore, the first order rate constant for diffusion of negative ions (equal to that of positive ions) would be approximately 14 sec^{-1}. Thus, even if negative ions do diffuse at the same rate as positive ions, k'_{IIR} is still about twice as large as k_d.

Ion-Ion Recombination

J.J. Thomson and E.R. Rutherford (27) were the first to recognize the importance of ion-ion recombination in 1896. Rutherford (28) made the first attempts to measure IIR rate constants in 1897 followed by Langevin (29) in 1903. However, these early experiments are thought to have very little validity due to the lack of vacuum and gas purification techniques at that time. It was not until the late 1930's that experiments became more reliable and the existence of three distinct pressure regimes in which the mechanism of IIR differ

was discovered (30).

Figure 1 shows how the IIR rate constant varies with pressure. At pressures below about 1 Torr, IIR occurs via a bimolecular mechanism. The rate constant for this process bears no dependence on pressure and typical experimental values are in the range of $9 \pm 5 \times 10^{-8}$ cm^3 sec^{-1} (30). Above about 1 Torr a termolecular mechanism takes over. From this pressure up to approximately 1 atm the IIR rate constant increases linearly with pressure. This behavior was predicted by Thomson (31) in 1924 and was first verified experimentally

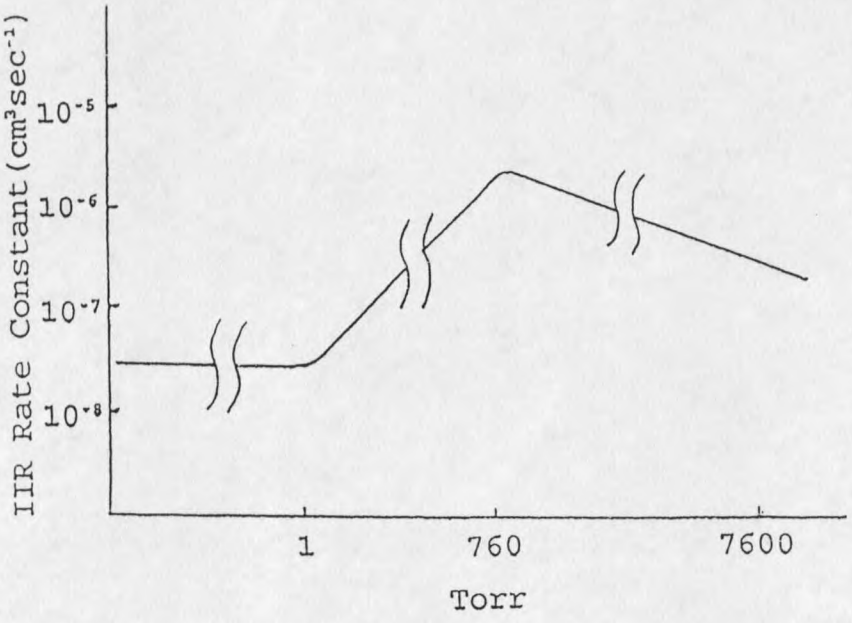

Figure 1. Plot of ion-ion recombination rate constant versus pressure.

by Sayers (32) and Gardener (33) in 1938. Near 1 atm the IIR rate constant reaches a maximum value of about 2 x 10^{-6} cm^3 sec^{-1} and then begins to decrease with increasing pressure. This phenomena was shown experimentally by Machler (34) and is explained by a theory proposed early on by Langevin (29) which states that the rate of IIR is limited by the speed at which the oppositely charged species can diffuse together.

Since the experiments of this thesis work were performed at or near atmospheric pressure, the termolecular mechanism for IIR will be discussed in greater detail below.

Termolecular Ion-Ion Recombination

Thomson (31) proposed the first theory to explain the recombination of ions in a high pressure ionized gas. This theory provided the fundamental basis for all subsequent recombination theories.

Thomson's theory considers two ions, one of charge e and the other of charge -e. These ions are assumed to be in thermal equilibrium with the gas, therefore, the average kinetic energy per ion is 3kT/2, where T is the temperature of the gas. The mutual potential energy of the ion pair is given by the Coulomb expression $-e^2/r$, where r is the separation

distance of the ions. The basis of the Thomson theory is that if the total relative energy of the ion pair ever becomes negative, recombination will occur. In other words, the kinetic energy of relative motion of the ions, W, must become less than the energy required to separate the ions by an infinite distance, ($W < e^2/r$), if recombination is to result (25). This condition cannot be met unless one of the ions collides with a third body. In the absence of third body collisions, the relative kinetic energy of the ions increases at the same rate as their mutual potential energy decreases, hence there is no net change in the total relative energy. However, if within a critical distance, r_c, one of the ions collides with a neutral, resulting in the return of that ion to the average thermal energy, the ions will become entrained in a closed orbit about each other and recombination will result. The critical radius comes from $3kT/2 = e^2/r_c$ and is given by Equation 13.

$$r_c = 2e^2/3kT \qquad (13)$$

Thomson's mechanism of recombination can be written in graphical notation by the reaction scheme shown below (35).

$$P^+ + N^- \rightarrow (P^+N^-)^* \quad (14)$$

$$(P^+N^-)^* \rightarrow P^+ + N^- \quad (15)$$

$$(P^+N^-)^* + M \rightarrow (P^+N^-) \rightarrow \text{neutrals} \quad (16)$$

Reaction 14 represents the ions approaching each other and entering a hyperbolic unbound orbit, denoted as $(P^+N^-)^*$. If one of the ions does not collide with a neutral while in this orbit, the ions will bypass each other and continue on their hyperbolic trajectory (Reaction 15). However, if an ion-neutral collision does occur, the ion pair may lose relative kinetic energy and become entrained in a bound elliptical orbit which results in recombination, shown by Reaction 16.

Thomson assumed that each ion is surrounded by a sphere of radius r_c, and that the sum of the number of collisions per second of oppositely charged ions within the ion sphere will equal the recombination rate. The number of ions entering the sphere is given by $\pi r_c^2 n^{\pm} [(v_m^+)^2 + (v_m^-)^2]^{1/2}$ where $n^{\pm}$ is the number of positive or negative ions per cm^3 and v_m represents the mean velocity of the ions. Then, if w is the probability that a collision between an ion and a neutral will occur within the sphere, the number of recombination events per cm^3 per sec is given by Equation 17.

$$R = \pi r_c^2 n^+ n^- [(v_m^+)^2 + (v_m^-)^2]^{1/2} (w^+ + w^-) \qquad (17)$$

The probability, w, is given (25) by $1 - \frac{\lambda^{\pm}}{2r_c}(1 - e^{-2r_c/\lambda^{\pm}})$ where $\lambda^{\pm}$ is the mean free path of the ion. Substituting this quantity for w and dividing by n^+n^- gives the ion-ion recombination rate constant in $cm^3\ sec^{-1}$.

Thomson's theory has several shortcomings, such as; neglecting the possibility of weakly bound ion pairs dissociating by subsequent collisions; that one ion-neutral collision within the critical radius may not result in unit probability of recombination; ignoring ion pairs with ionic separations greater than r_c; and failing to correctly predict the pressure dependance of the rate of IIR at pressures above about 2 atm. Subsequent theories (36), (37), (38), (39) have corrected for these problems and addressed other microscopic details of the physics involved in IIR. These theories are beyond the scope of this thesis. It should be noted however, that Thomson's theory still provides the best quantitative agreement with experimental results in the 0.1 to 1 atm pressure range and the mechanism shown in reactions 14-16 is still the fundamental way in which IIR is described.

EXPERIMENTAL

The Reaction/Dummy Cell Apparatus

A schematic of the reaction/dummy cell apparatus is shown in Figure 2. The flowing sections describe main components of the apparatus.

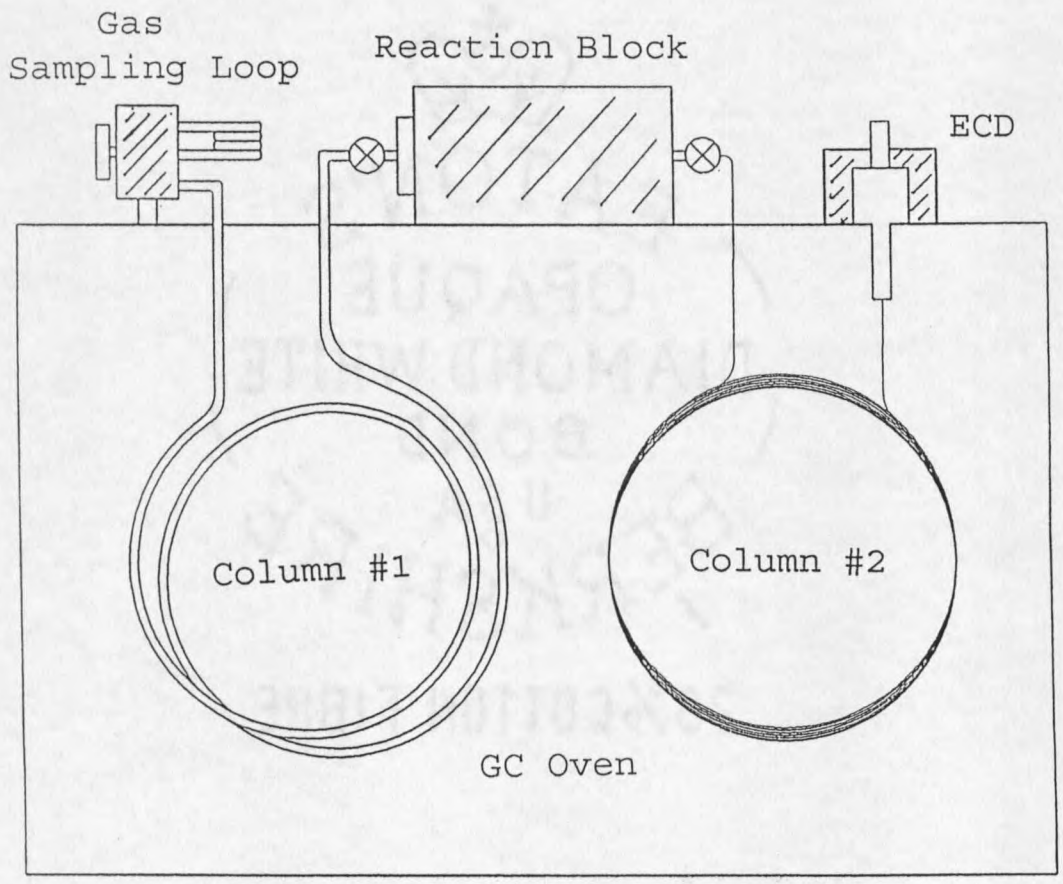

Figure 2. Schematic of reaction/dummy cell apparatus.

The Reaction/Dummy Cell

The reaction/dummy cell, shown in Figure 2, was constructed from a stainless steel block with dimensions of 8 cm(L) x 4cm(W) x 5cm(H). Within the block are two cylindrical cells 1.9 cm long and 1 cm in diameter, resulting in a volume of 1.5 cm^3 each. The wall of the reaction cell was formed by a 13 mCi ^{63}Ni-on-Ni foil, while that of the dummy cell was a non-radioactive Ni foil. The GC carrier flow could be selected to pass through either the reaction or dummy cell by use of an eight-way switching valve (Carle Model 2013), while the cell not selected was continuously purged with nitrogen. The temperature of the cell block was maintained between 30 and 180°C by a cartridge heater and thermocouple feedback loop controlled by an Omega temperature controller (Model CN370). To ensure the temperature of the gas within the cell was actually the same as the temperature of the cell block, a separate thermocouple was inserted into the cell cavity and the temperature was measured by a separate temperature readout device. It was determined that the temperature of the gas was always within ±2°C of the temperature of cell block.

For some experiments it was necessary to reduce the thermal electron population in the reaction cell so that no

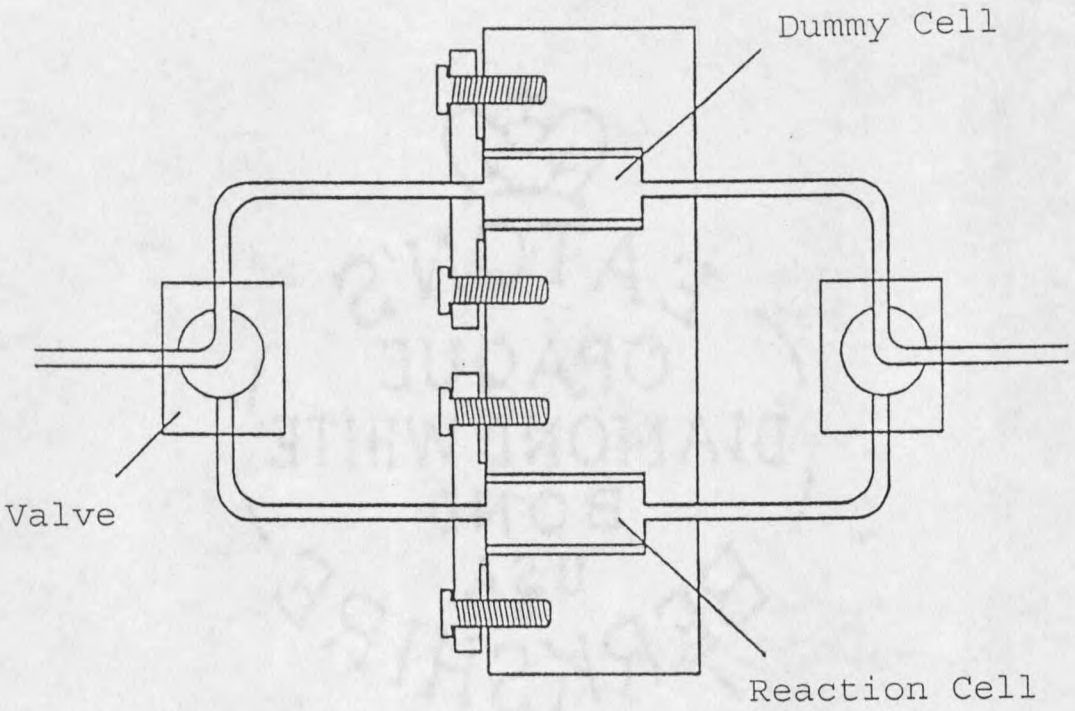

Figure 3. Reaction/dummy cell block.

more than about 90% of the compound being studied was destroyed by EC within the cell. This was accomplished by covering the ^{63}Ni foil with a stainless steel mesh that had only 2.5% open area, thereby reducing the effective activity of the foil to about 0.4 mCi. The pressure within the cells was 372 Torr above ambient due to the restriction created from chromatography column #2. This pressure was measured by installing a T fitting immediately after the cell but prior to column #2. A pressure gauge was then inserted through a septum in the fitting and the pressure measured in psi. The total absolute cell pressure was 1012 ± 10 Torr (or about 1.33 atm).

Sample Preparation and Introduction

All samples were obtained from commercial suppliers and were used without further purification since the chromatography provided separation from any impurities. All nitrobenzene (NB) and substituted analog samples were prepared in HPLC-grade toluene. An aliquot was taken from a stock solution of approximately 10.0 mg cm^{-3} and diluted to 1.0 cm^3 to make a final working solution of $1x10^{-4}$ mg cm^{-3}. For all other compounds, gas samples were prepared in nitrogen by injection of known quantities of the pure compounds into gas-

tight glass containers followed by appropriate dilutions. A 4.1 L carboy pressurized to 517 Torr above ambient was used for final storage of the compound. This allowed many samples to be removed while still maintaining a positive pressure within the carboy.

Samples were introduced into the reaction/dummy cell apparatus by one of two methods. For liquid samples, between 0.1 and 1.0 μl of sample was injected into a heated injection port on the GC (Hewlett Packard Model 5980). The sample then entered the reaction or dummy cell via an 18 meter by 0.53 mm SE-54 (Alltech) capillary column (column #1) that was heated to the appropriate temperature. A 12 meter capillary column of the same type (column #2) was used to transport the effluent from the cell to the ECD.

Gaseous samples were introduced to the GC by use of a six-way gas sampling valve (Carle Model 8030) equipped with a 0.25 cm^3 sample loop. The samples were transferred from the pressurized carboy to the gas sampling valve by a 50 cm^3 gas-tight glass syringe. Typically, between 5 and 30 cm^3 of sample was drawn into the syringe and then diluted to 50 cm^3 with nitrogen. This method allows the sample concentration to be varied without the need to make different carboys. A 10 ft by

1/8 in stainless steel column packed with 10% SF-96 on Cromosorb W (Alltech) was used as column #1 for all compounds except C_7F_{14}, C_6F_{12}, and SF_6. A 25 ft column of the same type was used for C_7F_{14} and C_6F_{12} while a 10 ft by 1/8 in stainless steel column packed with 5A molecular sieve was used for SF_6. Column #2 was the same as above. Both columns were maintained at 30°C.

The GC carrier gas was nitrogen that was first passed through oxygen, water, and molecular sieve traps. The carrier gas flow rate was 32 cm^3 min^{-1} as measured at the exit of the ECD. It was also necessary to know the flow rate through the reaction/dummy cell. This flow was calculated by Equation 18,

$$F_1 = F_2(P_1/P_2) \tag{18}$$

where F_1 is the flow rate through the reaction/dummy cell, F_2 is the flow rate measured at the ECD exhaust, P_1 is the pressure within the cell and P_2 is local ambient pressure. Using the above mentioned values for F_2, P_1, and P_2, the flow through the reaction/dummy cell was 19.4 cm^3 min^{-1}.

Detection of Compounds

The amount of compound of interest surviving passage through either cell was detected by an ECD. The ECD is a

commercial detector supplied with the GC. It is of the constant current type and is equipped with a 15 mCi ^{63}Ni foil. Pairs of chromatograms were then obtained, first with the GC carrier gas flow passing through the dummy cell and then with the flow passing through the reaction cell. In these paired analyses, the ratio of peak area responses is of fundamental interest. However, since peak heights were found to be proportional to their respective peak areas, the ratios of peak heights were used as a measure of response ratios. Paired analyses of this type were repeated at least three times for each compound of interest at each temperature of interest. The reproducibility of these repeated measurements was very good (peak height ratios varied by less than ±5%). Care was taken to use only very small sample sizes (generally less than 2 parts per billion in nitrogen), where changes in the amount of sample injected did not change the measured response ratios. Under these small sample conditions, only a small fraction of the electron population within the reaction cell is consumed as the EC active compound passes through the cell, thereby ensuring that the total electron population with the reaction cell remains relatively constant at all times (5).

For some experiments it was necessary to add

trimethylamine (TMA) to the carrier gas flow in order to change the nature of the positive ions within the reaction cell. This was accomplished by the injection of gaseous TMA into a 1.0 L stainless steel dilution vessel that was inserted in the carrier gas flow stream immediately ahead of the GC. The concentration of TMA in the nitrogen carrier gas varied from about 1 part per million up to about 1 part per thousand. The addition of TMA had no detrimental effect on the ECD standing current or on the electron density within the reaction cell.

The Dual Cell ECD

The dual cell ECD is shown in Figure 4. The dual cells were constructed from stainless steel and are of a concentric coaxial design. The cylindrical walls are formed by two matched 15 mCi ^{63}Ni-on-Pt foils. The volume of the cells are 2.2 cm^3 each and are separated by a 2 mm aperture which allowed unrestricted gas flow from one cell to the other. The electrons in the ECD's were collected by applying a fifty volt positive polarity pulse of 1.0 μsec duration to the axial pin in each cell every 50 μsec while the rest of the cell was electrically grounded. The two current signals were then

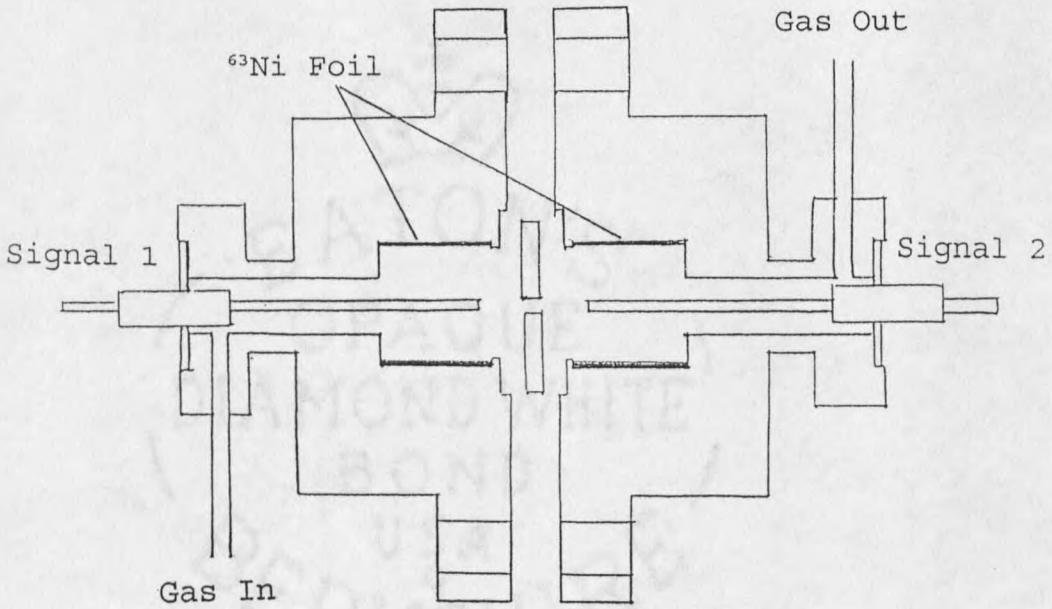

Figure 4. The dual cell ECD.

processed by an electronics package described in detail by Knighton and Grimsrud (40). As the compound of interest enters cell #1 EC occurs and the response is measured at pen #1 of a two pen chart recorder. The fraction of compound surviving passage through the first cell passes into cell #2, where part or all of the fraction will undergo EC and be recorded by pen #2. The responses were also sent to a microcomputer that was interfaced to the dual cell by the Montana State University Laboratory Interface. Integration of the peaks was accomplished with the computer and were double checked by cutting and weighing or by use of a planimeter.

The carrier gas was 10% methane in argon that was passed through purifying traps. Chromatography and sample introduction was the same as for the reaction/dummy cell experiments described above.

The Atmospheric Pressure Ionization Mass Spectrometer

Figure 5 shows the main components of the Atmospheric Pressure Ionization Mass Spectrometer (APIMS). It consists of an ion source, expansion chamber and a mass analyzer which has been described in detail by Grimsrud and coworkers (41),(42).

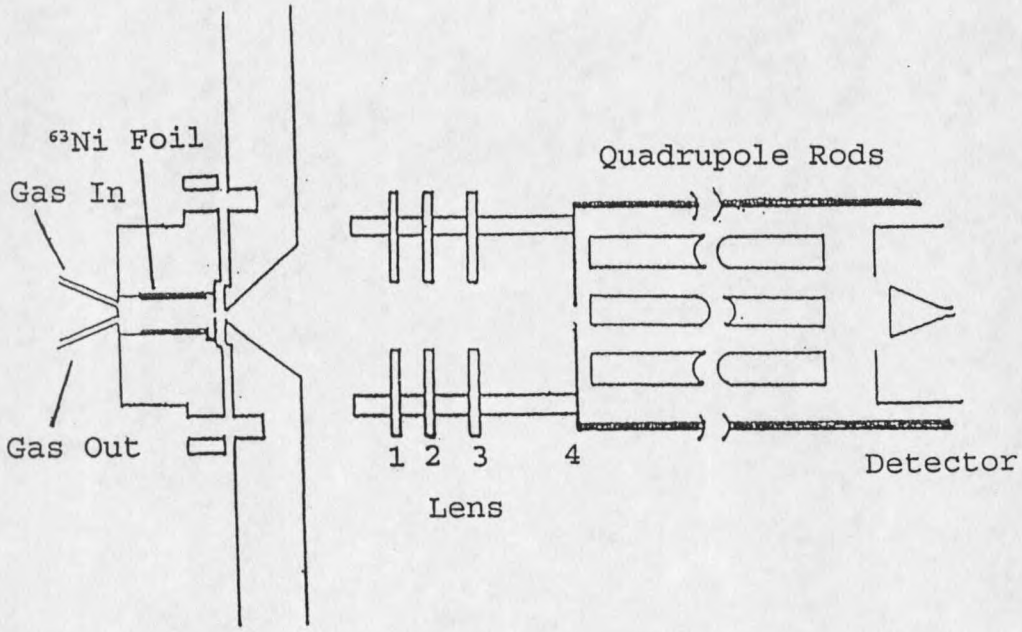

Figure 5. The Atmospheric Pressure Ionization Mass Spectrometer.

Major Components of the APIMS

The ion source was constructed from stainless steel and has a volume of 1.5 cm^3. The walls of the source are formed by a 15 mCi ^{63}Ni-on-Pt foil and the chemistry within the ion source is the same as that described for the reaction/dummy cell in the Theory section. In addition to the nitrogen gas flow from a chromatography column (about 20 $cm^3\ min^{-1}$), a make-up gas flow was added immediately after the column so that a total flow of approximately 50 $cm^3\ min^{-1}$ could be maintained through the ion source. A 50 μm aperture allowed passage of approximately 20 $cm^3\ min^{-1}$ of gas from the ion source into the expansion chamber, which is the first stage of a differentially pumped vacuum envelope. Once in the expansion chamber, any ions entrained in the gas are focused via lenses, L, 1 through 4 (lens potentials; L1 = 24V, L2 = 24V, L3 = 0V, L4 = 24V) onto the 2mm entrance aperture of the second differentially pumped region that contains a quadrupole mass filter. The quadrupoles could be scanned in the normal way to obtain a mass spectrum between 0 and 500 amu, manually tuned for single ion monitoring, or used in the rf only mode to monitor the total ion signal. An on-axis channeltron electron multiplier was used for ion detection. When sample

concentrations were sufficiently high that detector saturation occurred, it was sometimes necessary to defocus the ion beam using lense #3 (increasing its potential) such that changes in ion intensity could be monitored.

Sample Introduction

Samples were introduced to the APIMS ion source by several different methods, including a gas sampling valve, a dilution vessel and by "direct" injection. Introduction via a gas sampling valve has already been described. A 1 liter stainless steel dilution vessel was used when a continuous flow of a compound into the ion source was needed. For example, when the positive ions within the ion source wanted to be changed, 1μl of triethlyamine (TEA) liquid was injected into a dilution vessel which was inserted in the make-up gas line. The TEA concentration remained sufficiently high over time such that numerous experiments could be performed. Lastly, some samples were injected directly into the make-up gas line through a septum in a T fitting. This was done when a large amount of a known pure compound was needed in the ion source.

RESULTS AND DISCUSSION

Relative Ion-Ion Recombination Rate Constants

Because IIR is the dominant loss mechanism of ions in a high pressure ionized gas, it is of fundamental importance to know the rate at which IIR occurs in order to understand and predict the chemistry of ionized gases. Of the small number of studies that have determined rate constants of termolecular IIR, none have fully investigated the effect of differing the recombining ions. Therefore, it has always been assumed that the nature of the recombining ions has no effect on the rate of IIR. In addition, no experiments have ever been performed in which the identities of the ions have been monitored simultaneously with the measurement of IIR rates.

Studies by McGowan (24) in which a nitrogen buffer gas was doped with oxygen showed that at 760 torr and 25°C, the IIR rate constant was about 2.2×10^{-6} cm^3 sec^{-1}. The ions were assumed to be NO^+, O_4^+, NO_2^-, and O_2^-. This is in good agreement with Sayers' (32) value of 2.3×10^{-6} for air and Gardner's value of 2.1×10^{-6} for pure oxygen. Mahan (35) has also

determined IIR rate constants with nitrogen oxide (NO) in various buffer gases at pressures between 10 and 600 Torr. These results showed that the rate constant increased with increasing pressure, as predicted by Thomson's theory, reaching a maximum value of approximately 1.2 x 10^{-6} to 1.4 x 10^{-6} cm^3 sec^{-1} in the heavier buffer gases (N_2, Ar, Xe, Kr).

Presently, the most widely accepted rate constant for IIR is 2.0 x 10^{-6} cm^3 sec^{-1}. This value is typically used for all IIR reactions in the vicinity of 1 atm pressure. Experiments performed for this thesis, described in the following paragraphs, account for the inadequacies of previous experiments by positively identifying the recombining ions as well as varying the nature of the ions.

The APIMS was used to investigate IIR reactions in the following manner. First, all positive ion chemistry was controlled by the addition of triethylamine to the atmospheric pressure buffer gas. Second, the negative charge side of the plasma was saturated by the addition of strongly electron attaching compounds. Lastly, the intensity of the positive ion signal was monitored while the electron attaching compound flowed through the ion source. A detailed explanation of this procedure is given below.

Positive Ions

Reactions 19a and 19b are the primary ionizing events in nitrogen buffer gas (43).

$$\beta + N_2 \rightarrow N_2^+ + 2e^- \quad (75\%) \quad (19a)$$

$$\beta + N_2 \rightarrow N^+ + N + 2e^- \quad (25\%) \quad (19b)$$

The subsequent clustering reactions, shown in reactions 20a and 20b are sufficiently fast compared to recombination with

$$N_2^+ + 2N_2 \rightarrow N_4^+ + N_2 \quad (20a)$$

$$N^+ + 2N_2 \rightarrow N_3^+ + N_2 \quad (20b)$$

electrons and charge transfer to impurities, that N_4^+ and N_3^+ are considered pseudo-primary ions which will have lifetimes on the order of several milliseconds (22). In that time period at atmospheric pressure, an ion will undergo approximately 5 x 10^6 collisions. Therefore, the terminal positive ions may be the reaction products of pseudo-primary ions with buffer gas impurities that are present at 1 ppm or greater. If a dopant is added to the buffer gas at concentrations of 10-100 ppm, the first collisions the pseudo-primary ions will experience will be with dopant molecules (44).

In order to create a fixed, stable set of positive ions within the APIMS ion source, approximately 1.0 μl of

triethylamine (TEA) was injected into a stainless steel dilution vessel that was inserted in the nitrogen make-up gas line. TEA is thought to undergo reactions 21a-c to give the terminal positive ions shown in Figure 6.

$$N_4^+ + (CH_3CH_2)_3N \rightarrow (CH_3CH_2)_2NCH_2^+ + 2N_2 + CH_3 \quad (21a)$$

$$N_4^+ + (CH_3CH_2)_3N \rightarrow (CH_3CH_2)_2NCH_2CH_2^+ + 2N_2 + H \quad (21b)$$

$$N_4^+ + (CH_3CH_2)_3N \rightarrow (CH_3CH_2)_3N^+ + 2N_2 \quad (21c)$$

$$(CH_3CH_2)_3N^+ + (CH_3CH_2)_3N \rightarrow (CH_3CH_2)_3NH^+$$

The intensity ratios of the $(M-CH_3)^+$, $(M-H)^+$, and $(M+H)^+$ ions are 0.30 : 1.0 : 0.75 and are reflective of their relative reaction rates. The ion at mass 187 in Figure 6 is due to the cluster ion $(M-CH_3^+)\cdot M$. The ratio of the $(M+H)^+$ to $(M-H)^+$ and $(M-CH_3)^+$ ion increases with decreasing concentration of TEA in the ion source. This is because of the increasing probability that the first reactive collision will be with water, which is present at background levels of about 1 ppm. Reaction sequence 22 shows the mechanism for $(M+H)^+$ formation involving water.

$$N_4^+ + H_2O \rightarrow H_2O^+ + 2N_2 \quad (22a)$$

$$H_2O^+ + n\ H_2O \rightarrow H_3O^+(H_2O)_{n-1} + OH \quad (22b)$$

$$H_3O^+(H_2O)_x + (CH_3CH_2)_3N \rightarrow (CH_3CH_2)_3NH^+ + H_2O \quad (22c)$$

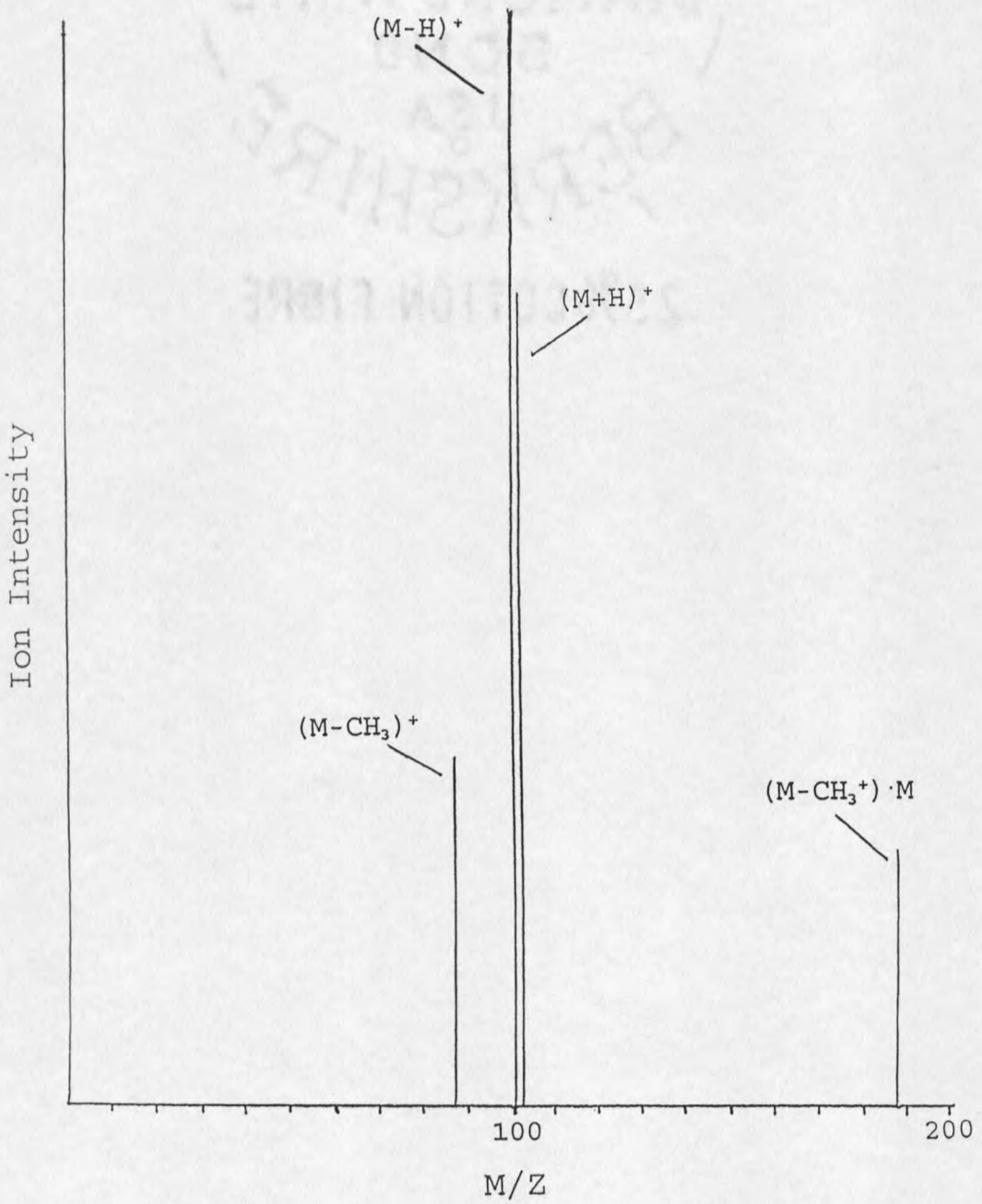

Figure 6. API mass spectrum of triethylamine at 120°C in nitrogen buffer gas shortly after 1μl was injected into the dilutor.

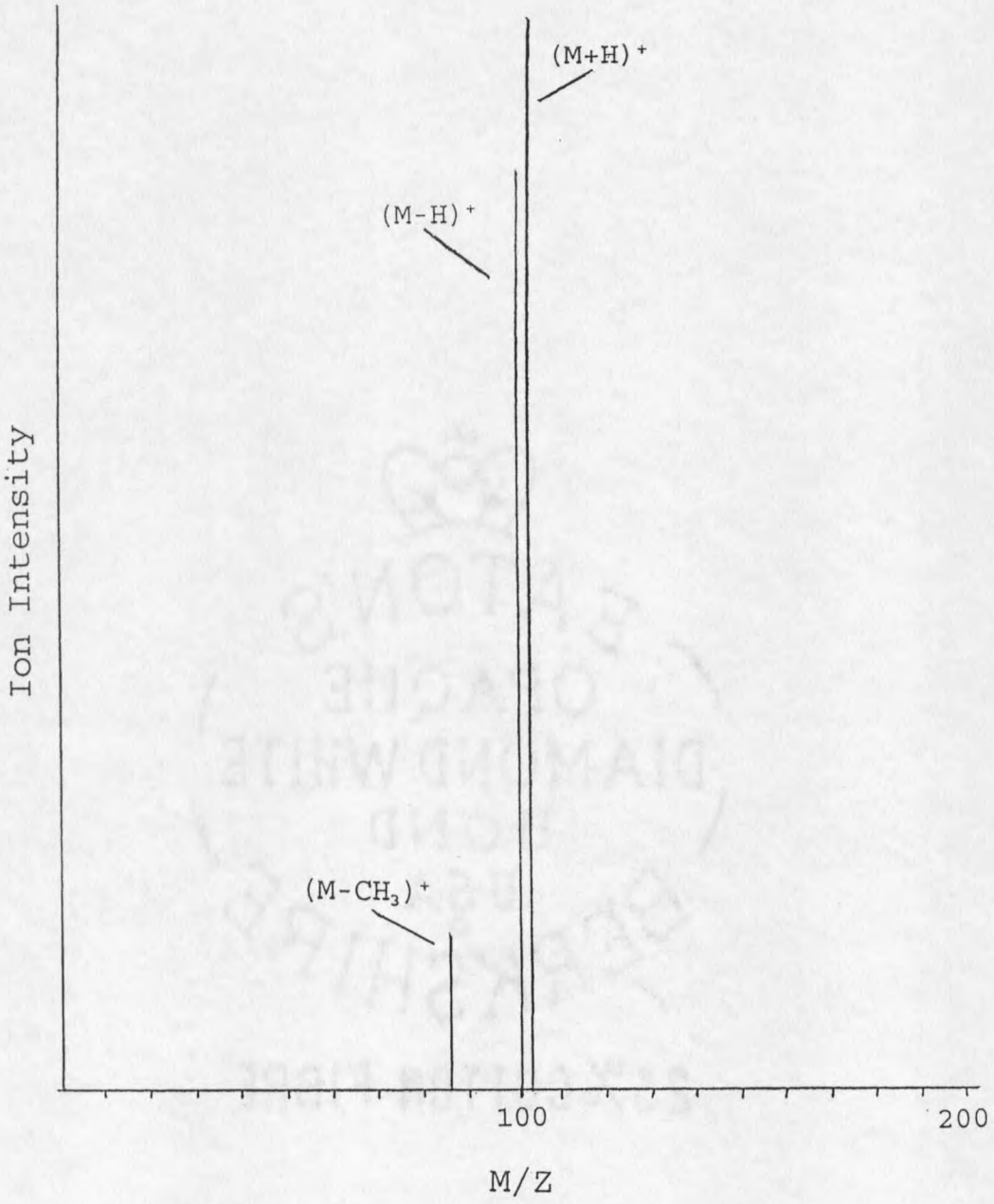

Figure 7. API mass spectrum of triethylamine approximately two hours after it was injected into the dilutor.

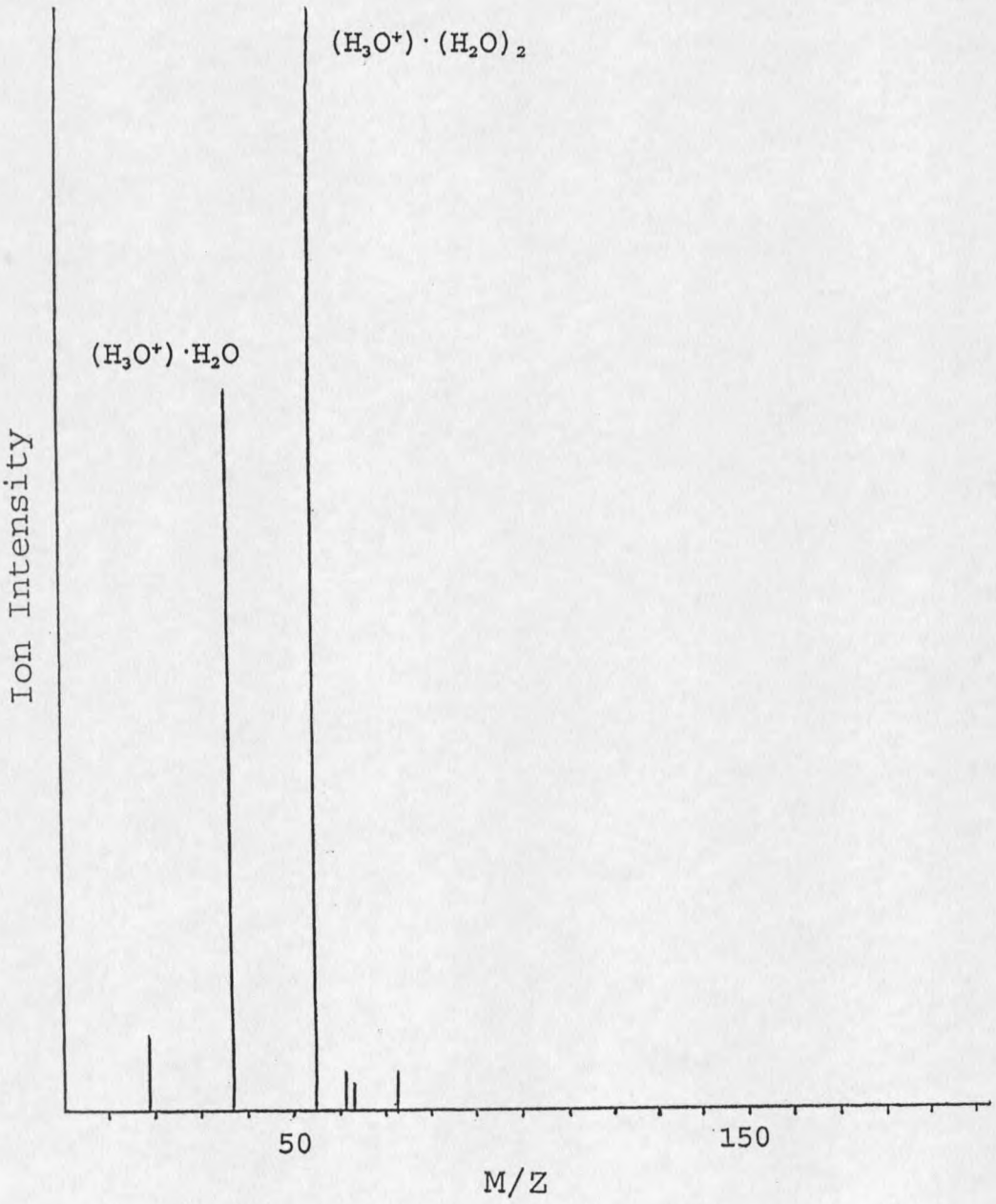

Figure 8. API positive ion background mass spectrum.

Approximately two hours after the initial injection of TEA, the $(M+H)^+$ to $(M-H)^+$ ratio stabilized and the cluster ion at mass 187 disappeared, as shown in Figure 7. With a flow of 20 cm^3 min^{-1} through the dilutor and an initial concentration of 200 ppm, the concentration of TEA in the dilutor after two hours was estimated to be 18 ppm.

For comparison, the APIMS background positive ion mass spectrum is shown in Figure 8. It consists of two major ions at mass 37 and 55, which are water clustered hydronium ions with one and two water molecules respectively. These ions are formed via Reactions 22 a-b.

Negative Ions

To assure that the negative charge side of the plasma was saturated with the ions of interest, successive amounts of the appropriate compound were introduced into the ion source until the negative ion signal no longer increased. The ions of interest, Cl^-, Br^-, I^-, SF_6^-, and $C_7F_{14}^-$, were produced from electron capture to $CFCl_3$, CF_3Br, CH_3I, SF_6, and C_7F_{14} respectively. Due to the large amount of compound necessary to achieve saturation, chromatographic introduction was not possible. Therefore, all compounds were injected in their pure

form directly into the make-up gas line. Sample sizes were as follows; 20 μl $CFCl_3$ headspace, 5 μl CF_3Br, 1 μl CH_3I headspace, 1 μl SF_6, and 5 μl C_7F_{14} headspace. Prior chromatographic analysis of these compounds showed no impurities.

Interpretation of Data for Relative IIR Rate Constants

Once the positive ions were fixed and stabilized (about two hours after injecting the TEA) the APIMS was placed in the "rf only" mode, which allowed passage of all positive ions through the quadrupole mass filter. The total positive ion signal was then monitored during the introduction of the strongly electron attaching compound. The intensity of the total positive ion signal is proportional to $(S/R)^{1/2}$ (Equation 4). Thus, by knowing the difference in the positive ion signal between the case in which no EC active compound is present to the case where the ion source is saturated with negative ions, it is possible to determine the relative IIR rate constants. As can be seen in Table 1, the percent increase in the positive ion signal was about the same no matter which EC active compound was introduced into the ion source.

Table 1.

APIMS total positive ion signal during the introduction of electron attaching compound.

Negative Ion	$P_0 \times 10^{-5a}$	$P_s \times 10^{-5a}$	$P_0/P_s - 1$
Cl^-	2.16	2.80	0.30
Br^-	2.35	3.15	0.34
I^-	1.85	2.50	0.35
SF_6^-	1.78	2.40	0.35
$C_7F_{14}^-$	1.72	2.25	0.31

[a] Units are counts sec^{-1}

Since P_s, the positive ion signal when the ion source was saturated with negative ions, is greater than P_0, the positive ion signal in the absence of an EC active compound, IIR is slower than positive ion-electron recombination. The percent change in the positive ion signal should be proportional to the difference in the rate constants for the two recombination processes. Using 3×10^{-6} cm^3 sec^{-1} for the positive ion-electron recombination rate constant (23), and 33% as the average increase in positive ion signal, the IIR rate constant is calculated to be 2.0×10^{-6} cm^3 sec^{-1}. This is in excellent agreement with the previous results listed at the beginning of this section. These results also demonstrate that the nature

of the recombining ions has essentially no effect on the IIR rate constant.

Fate of Selected Molecular Anions Upon Recombination with Positive Ions

Only two reports exist in the literature that offer experimental evidence for the products formed in IIR reactions involving polyatomic ions. The first of these was a study of the reaction, $NO^+ + NO^- \rightarrow$ products, by Smith et al. (45) in which emitted optical radiation indicated the formation of electronically excited NO. These results were obtained using a flowing afterglow apparatus operating at 0.5 Torr in helium buffer gas. The other report by Valkenburg et al. (46) is particularly relevant to this thesis work. The object of their study was to determine the fates of the molecular anions of SF_6 and C_7F_{14} upon recombination with positive ions in an atmospheric buffer gas (10% methane in argon). Their experiment was based on a comparison of the two responses observed when small amounts of SF_6 and C_7F_{14} were passed through the same dual cell ECD shown in Figure 4. The ratio of these two responses were interpreted in terms of the extent to which the original molecule was lost by EC and then

regenerated by IIR. The intriguing conclusions of that investigation were that the molecular anions of C_7F_{14} were converted primarily back to the original molecule, C_7F_{14}, upon recombination with positive ions, while the molecular anions of SF_6 appeared to be converted primarily to altered neutral products. In arriving at these conclusions, Valkenburg et al. had to make two critical assumptions concerning potential sources of error that could not be directly proven by their experiment. The first of these assumptions was that only the parent SF_6 and C_7F_{14} molecules contributed significantly to the ECD responses observed by the dual cell ECD's (that is, it was assumed that any altered neutrals produced by IIR reaction 2b did not contribute significantly to the ECD responses). The second assumption was that the literature values for the EC rate constants of SF_6 and C_7F_{14}, determined by Smith et al. (16) and by Alge et al.(17) in helium buffer gas at 0.5 Torr, would also apply to EC reactions in 10% methane in argon buffer gas at 1.0 atm pressure.

While the reports of Smith et al. (45) and Valkenburg et al. (46) have provided a significant beginning in the attempt to experimentally reveal the products of IIR reactions, additional experimental methods for the characterization of

these elusive processes are clearly needed. Therefore, the experiments to be described here use a different and more definitive experimental approach to study the EC and IIR reactions of many compounds, including the ones studied by Valkenburg et al.(46).

Treatment of the Data

The reaction/dummy cell apparatus, shown in Figure 2, was used to determine the fates of molecular anions upon IIR. In a ^{63}Ni ionization source of this type (the reaction cell), a population of electrons and positive ions will be continuously maintained throughout its volume (47) as nitrogen buffer gas is passed through it at a pressure of 1.33 atm. As small amounts of a compound, M, are passed through the reaction cell, reactions 1 and 2a/b will occur. Because the dimensions of the reaction cell are large relative to the diameter of its entrance and exit ports, a compound entering the cell with the carrier gas flow will tend to be well mixed throughout the reaction volume so that a single expression, [M], can be used to describe its steady state concentration. The following conservation equation can then be written for the production and loss of M within the reaction cell:

$$\frac{F}{V}[M]_0 + \chi R \frac{N_{P^+}}{V}\frac{N_{M^-}}{V} = \beta \frac{N_e}{V}[M] + \frac{F}{V}[M] \qquad (23)$$

where F is the volumetric gas flow through the reaction cell, V is the volume of the cell, $[M]_0$ is the concentration of M in the gas stream that is flowing into the reaction cell, χ is the fraction of recombination events that lead to the regeneration of M (as in reaction 2a), N_{P^+}, N_{M^-}, and N_e are the number of positive ions, molecular anions, and electrons, respectively, within the reaction cell, R is the IIR rate constant, and β is the EC rate constant for M. The two terms on the left side of Equation 23 describe the rate of production of M by flow into the reaction cell and by IIR (reaction 2a), while the two terms on the right side describe the rate of loss of M by EC and by flow out of the cell.

Another conservation equation for the production and loss of the negative ion, M^-, is given by Equation 24:

$$\beta \frac{N_e}{V}[M] = R \frac{N_{P^+}}{V}\frac{N_{M^-}}{V} \qquad (24)$$

where the left side describes the production of M^- by EC and the right side describes the loss of M^- by IIR. As was explained in the Theory section, ventilation and diffusion are considered negligible loss mechanisms.

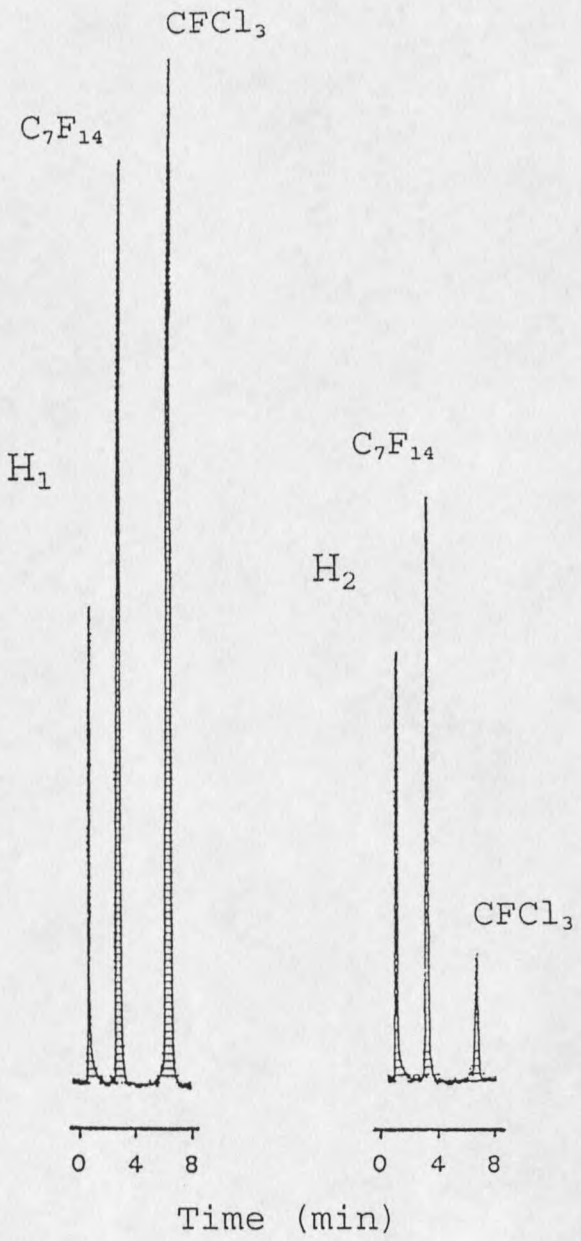

Figure 9. Typical GC-ECD analysis of a gas sample containing about 1.5 ppb $CFCl_3$ and 1.0 ppb C_7F_{14} in nitrogen obtained with the reaction/dummy cell apparatus at 120°C. The chromatograms labeled H_1 were obtained with the carrier gas passing through the dummy cell, while those labeled H_2 were obtained with the carrier gas passing through the reaction cell.

Figure 9 shows an example of the paired chromatograms obtained when the reaction/dummy cell apparatus was used. Chromatogram H_1 was obtained with the carrier gas passing through the dummy cell, while chromatogram H_2 was obtained with the carrier gas passing through the reaction cell. The peak heights observed when the dummy cell is used will be proportional to the quantity $[M]_o$, since no destruction of M is expected in the dummy cell. Similarly, the peak height when the reaction cell is used will be proportional to the quantity [M]. The resulting relationship, $H_1/H_2 = [M_o]/[M]$, combined with Equations 23 and 24 above, yield Equation 25:

$$(1-\chi)\beta = \frac{F}{N_e}\left(\frac{H_1}{H_2}-1\right) = \alpha \qquad (25)$$

where the middle term is a combination of experimentally determined factors that will hereafter be collectively represented by the symbol, α.

The number of electrons in the reactor cell, N_e, was determined by use of the reference compound, $CFCl_3$, for which β values have been previously determined over the temperature range of interest here (16). For compounds such as $CFCl_3$, that undergo EC by the dissociative mechanism ($e + CFCl_3 \rightarrow CFCl_2 + Cl^-$), the original molecule, $CFCl_3$ cannot possibly be

regenerated by an IIR reaction. Therefore, for this compound, $\chi = 0$ and $\alpha = \beta$ (from Equation 25) can be assumed. Since β and α for $CFCl_3$ are known and the flow rate, F, was determined to be 0.34 cm^3 sec^{-1}, the magnitudes of N_e were determined at each temperature by Equation 25 using measurements of H_1/H_2 for this reference compound. The uncertainty of these N_e determinations was essentially equal to that of the literature β values for $CFCl_3$, about $\pm$ 25%. This same level of uncertainty applies to the α values obtained from the measured parameters, including N_e, shown in Equation 25.

From the values of α thereby measured for the compounds studied and from independently determined values of β, the magnitude of χ for these compounds was then determined by Equation 26.

$$\chi = 1 - \frac{\alpha}{\beta} \tag{26}$$

The uncertainty in χ, (s_χ), is derived by applying the standard method for propagation of errors (48), and is shown in Equation 27:

$$s_\chi = \frac{1}{\beta}\sqrt{s_\alpha^2 + \left(\frac{\alpha}{\beta}\right)^2 s_\beta^2} \tag{27}$$

where s_α and s_β are the uncertainties in α and β respectively.

Measurement of EC Rate Constants
at Atmospheric Pressure

As was demonstrated in the previous section, the EC rate constant for the compound of interest must be known to determine the regeneration coefficient, χ. The critical question as to whether or not the literature EC rate constants for C_7F_{14} that were determined in a buffer gas of 0.5 Torr (17) are applicable to buffer gas pressures near 1 atm must be addressed. In order to answer that question, experiments were performed using the dual cell ECD shown in Figure 4. The dual ECD's were used for the GC detection and analysis of samples containing $CFCl_3$, CCl_4, and C_7F_{14}, in which two responses were simultaneously recorded with 10% methane in argon carrier gas flowing through the ECD's at atmospheric pressure. The average electron density within each of the ECD's can be controlled by the choice of pulse frequency applied to their anodes. For this study, a very low average electron density (about 1×10^6 cm^{-3}) was maintained at all times (46) by setting the pulse frequency to a relatively high value of 5×10^5 Hz. As a result, only small fractions of the EC active compounds are destroyed by EC and IIR reactions as they pass through the dual ECD's under these conditions. This was verified by the

observation that the responses of the second ECD to the compounds studied were only slightly less (less than 15%) reduced relative to those of the first ECD.

Since the fractional destruction of the EC active compounds introduced to the first cell is small, the instantaneous response of the first cell will be proportional to the product of β and $[M]_0$, where β is the EC rate constant for that compound and $[M]_0$ is the known concentration of that compound being introduced to the first ECD. Therefore, under these conditions, the relative molar responses (peak areas / moles injected) observed for the EC active compounds will be directly proportional to the relative EC rate constants for these compounds in the atmospheric pressure buffer gas.

For $CFCl_3$, CCl_4, and C_7F_{14}, the average relative ECD responses in the above experiments at a detector temperature of 120°C were 1.00, 1.18, and 0.34, respectively (normalized with respect to the case of $CFCl_3$). The EC rate constants determined for these three compounds by the flowing afterglow method in 0.5 Torr helium buffer gas at 120°C are 3.2×10^{-7}, 3.8×10^{-7} (16), and 1.1×10^{-7} (17) $cm^3\ sec^{-1}$ respectively. These EC rate constants are in excellent agreement with the relative ECD responses observed here in a buffer gas of 1 atm

pressure. For the case of $CFCl_3$ and CCl_4, this result was explicitly expected, since the EC mechanisms for these two compounds are dissociative and do not require participation by the buffer gas. Since the resonance EC mechanism of C_7F_{14} does require participation by the buffer gas, however, this result is of great significance in that it provides verification for the assumption that the EC rate constants for C_7F_{14} determined by Alge et al.(17) under low pressure conditions are, indeed, applicable to the present buffer gas conditions of near atmospheric pressure.

Experiments using the dual cell ECD's under the same operating conditions described above were also performed to verify the reaction/dummy cell experimental results in which EC rate constants for dissociatively attaching compounds were determined. It was also used to determine EC rate constants for compounds that undergo resonance EC which have not been previously reported.

χ Values for SF_6, C_7F_{14}, and C_6F_{12}

The results for the three perfluorinated compounds studied are summarized in Table 2. The first two compounds

Table 2.

Summary of results for SF_6, C_7F_{14}, and C_6F_{12} with CF_2Br_2 and $CHCl_3$ as method checks.

Compound	Temp (°C)	electron density	β (cm^3sec^{-1})[a]	H_1/H_2	α (cm^3sec^{-1})[c]	χ[d]
CF_2Br_2	30	$8.4x10^6$	$3.1x10^{-7}$	9.1	$3.3x10^{-7}$	0[e]
	75	$6.4x10^6$	$3.5x10^{-7}$	8.7	$4.1x10^{-7}$	0
	120	$4.0x10^6$	$3.8x10^{-7}$	6.4	$4.6x10^{-7}$	0
	180	$2.4x10^6$	$4.0x10^{-7}$	3.9	$4.1x10^{-7}$	0
$CHCl_3$	180	$3.4x10^6$	$1.7x10^{-8}$	1.15	$1.5x10^{-8}$	0[e]
SF_6	30	$1.2x10^7$	$3.1x10^{-7}$	10.4	$2.7x10^{-7}$	0.13±0.31
	75	$7.9x10^6$	$3.6x10^{-7}$	8.8	$3.3x10^{-7}$	0.08±0.32
	120	$6.5x10^6$	$4.0x10^{-7}$	7.5	$3.4x10^{-7}$	0.15±0.30
	180	$4.0x10^6$	$4.5x10^{-7}$	5.4	$3.7x10^{-7}$	0.17±0.28
C_7F_{14}	30	$1.6x10^7$	$6.8x10^{-8}$	1.60	$1.3x10^{-8}$	0.81±0.07
	75	$1.1x10^7$	$8.8x10^{-8}$	1.52	$1.6x10^{-8}$	0.82±0.06
	120	$8.7x10^6$	$1.1x10^{-7}$	1.50	$2.0x10^{-8}$	0.82±0.06
	180	$5.3x10^6$	$1.3x10^{-7}$	1.47	$3.0x10^{-8}$	0.77±0.08
C_6F_{12}	30	$1.6x10^7$	$1.6x10^{-7}$	3.17	$4.6x10^{-8}$	0.71±0.10
	75	$9.5x10^6$	$1.7x10^{-7}$	2.51	$5.4x10^{-8}$	0.67±0.12
	120	$6.9x10^6$	$1.8x10^{-7}$	2.30	$6.4x10^{-8}$	0.63±0.13
	180	$3.4x10^6$	$2.1x10^{-7}$	1.92	$9.4x10^{-8}$	0.56±0.16

[a] β is the electron capture rate constant obtained from references 16 and 49 as determined by the FALP method in 0.5 Torr buffer gas, except for C_6F_{12} which was determined by the present work with the dual cell ECD's at 1 atm pressure.

[b] H_1/H_2 is the ratio of peak heights, defined in Figure 4.

[c] α is the experimentally determined quantity defined in Equation 3.

Table 2. (continued)

[d] χ is the fraction of IIR events that lead to the regeneration of the parent molecule.

[e] For these dissociative EC processes, $\chi = 0$ is assumed.

shown, CF_2Br_2 and $CHCl_3$, provide a confirmation of the method because they are known to attach thermal electrons by the dissociative EC process. Therefore, χ for these compounds can be assumed to be equal to zero and the magnitude of α observed should be equal to the known (16),(49) EC rate constants, β (Equation 25). It is seen that α is, indeed, essentially equal to β for CF_2Br_2 and $CHCl_3$, thereby supporting the validity of the method. It is noted that the EC rate constant for $CHCl_3$ is much lower than that of CF_2Br_2 and, therefore, the ratio of peak heights, H_1/H_2, is only slightly greater than unity for this compound at 180°C. At lower temperatures, the EC rate constants of $CHCl_3$ are known to be even smaller and therefore, the H_1/H_2 values observed at lower temperatures were too close to unity to allow accurate determinations of α by Equation 3.

For SF_6, the observed values of α in Table 2 are almost equal to (slightly smaller than) the known β values for SF_6 at all temperatures studied. This leads to molecular regeneration

coefficients, χ, of less than 0.20 at all temperatures. This result indicates that SF_6^- is primarily converted to unknown neutral species upon recombination with positive ions and that less than 20% of the SF_6^- molecular anions are converted back to SF_6. These results are in good agreement with the value of $\chi = 0.1 \pm 0.3$ for SF_6^- previously reported by Valkenburg et al. (46) using 10% methane in argon buffer gas at 1.0 atm pressure and 150°C.

For C_7F_{14}, the observed values of α in Table 2 are distinctly smaller than (about 1/4 as large as) the known values of β for this compound at all temperatures. This leads to molecular regeneration coefficients, χ, that are close to 0.80 at all temperatures studied. This result suggests that $C_7F_{14}^-$ is primarily converted back to the molecular species, C_7F_{14}, upon recombination with positive ions and is also in very good agreement with the previous determination of $\chi = 0.75 \pm 0.10$ by Valkenburg et al. at 150°C.

An alternate explanation of the C_7F_{14} results has been considered. That is, these results would be explained if the rate constants for the resonance EC reaction of this compound under the present conditions of 1 atm. pressure are much lower (by a factor of 1/4) at all temperatures than the literature

values of β. As described in the previous section, however, experiments were performed in order to specifically test this possibility. In these experiments, it was shown that the relative EC rate constants for the reference compound, $CFCl_3$, and C_7F_{14} in an atmospheric pressure buffer gas are in excellent agreement with the corresponding literature values of β determined in 0.5 Torr helium buffer gas. Furthermore, it is difficult to envision how the rate constant of a thermal energy resonance EC reaction could be decreased, rather than increased, by an increase in pressure. For these reasons, this alternate explanation of the C_7F_{14} results is not favored.

The χ values for SF_6 and C_7F_{14} do not exhibit a significant temperature dependance. However, upon examination of the χ values of C_6F_{12} in Table 2, there is a clear decrease in χ as the temperature is increased from 30° to 180°C. At the lowest temperature of 30°C, a large amount of the parent molecule is regenerated upon IIR, while at 180°C, approximately 20% less of the parent molecule is regenerated.

In order to more precisely consider the significance of the χ values listed in Table 2 for SF_6, C_7F_{14}, and C_6F_{12}, it is informative to also consider the electron capture mass spectra of these compounds that were measured under the present

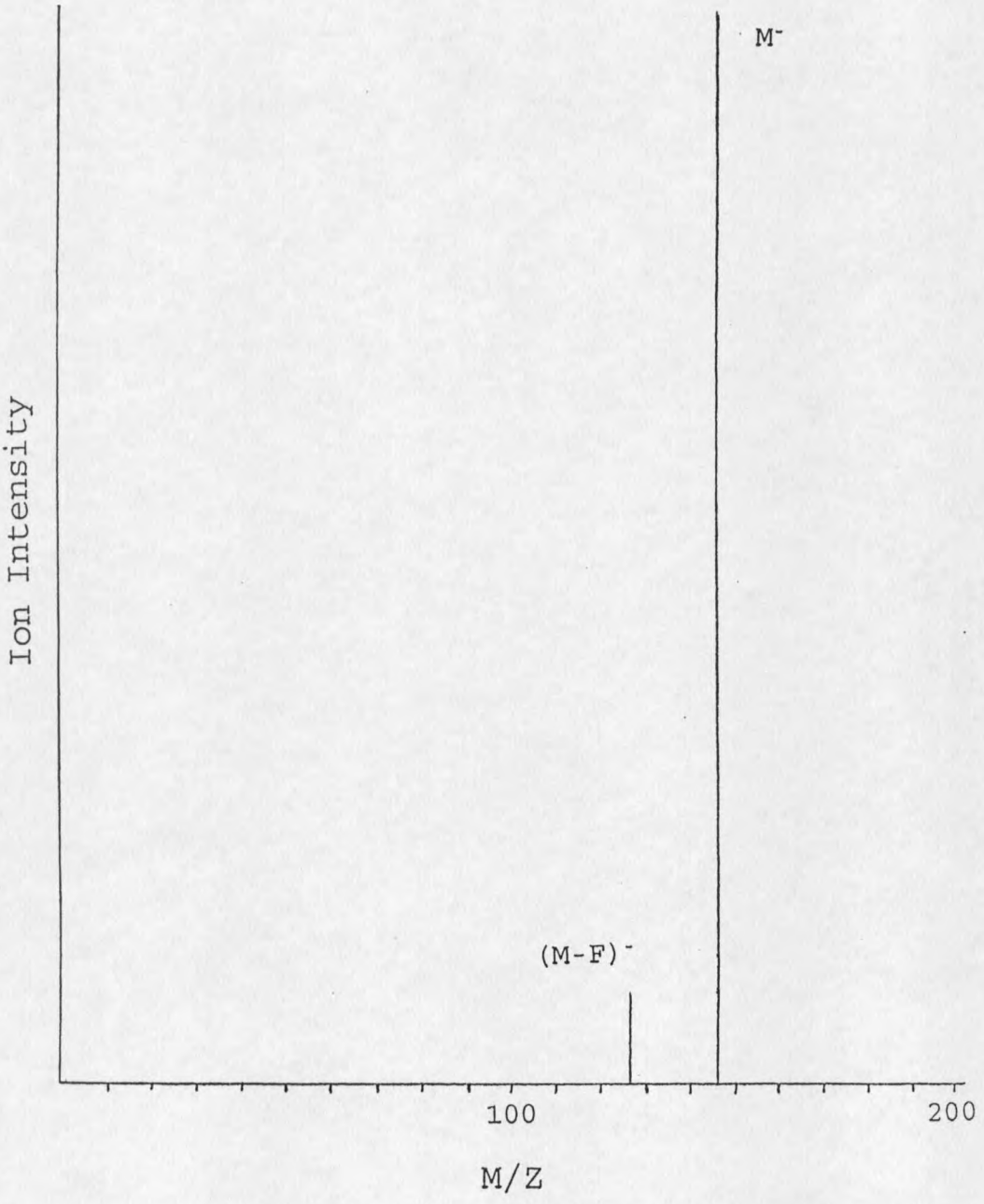

Figure 10. API mass spectrum of SF_6 at 120°C in nitrogen buffer gas.

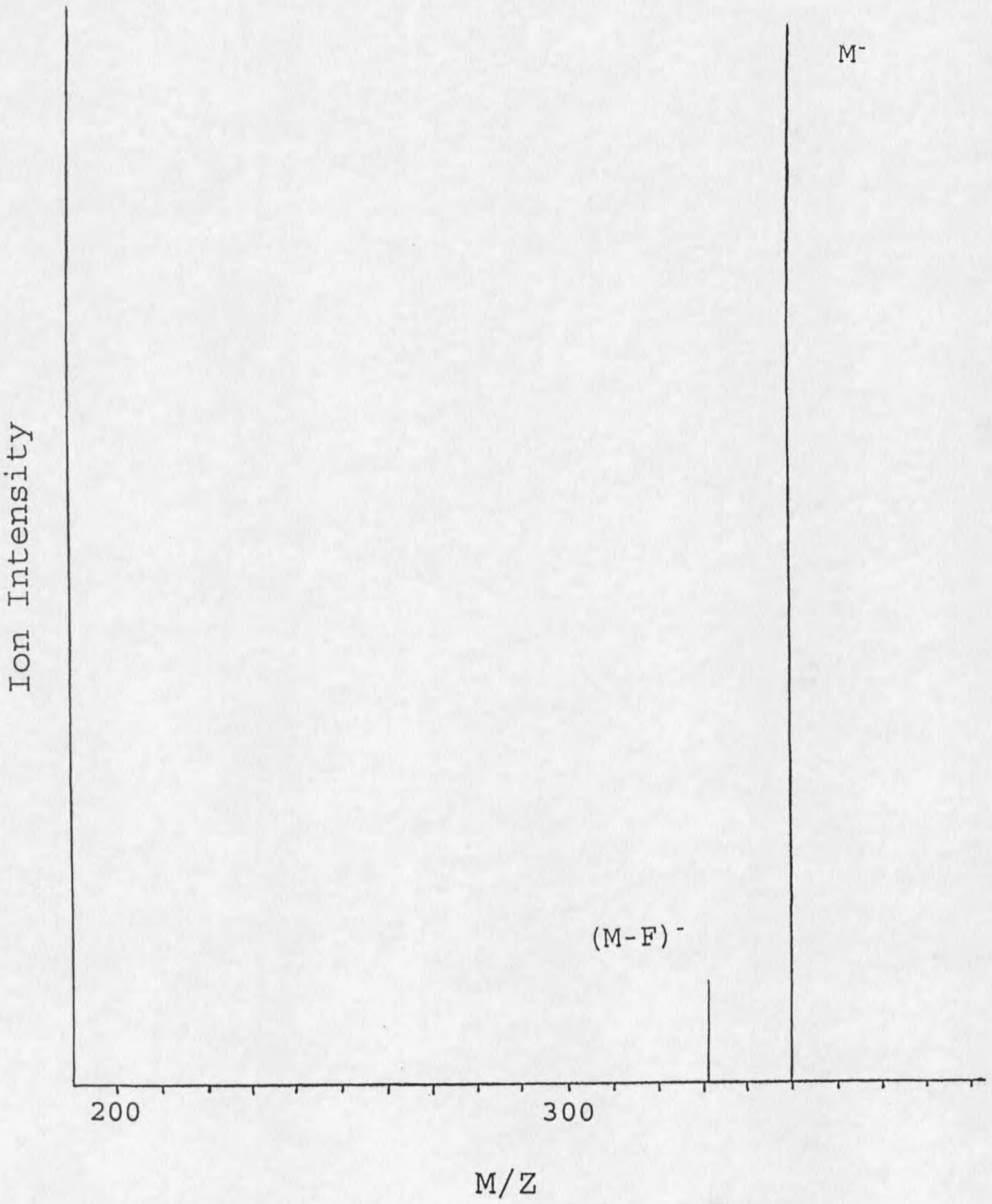

Figure 11. API mass spectrum of C_7F_{14} at 120°C in nitrogen buffer gas.

conditions by atmospheric pressure ionization mass spectrometry (APIMS). First, SF_6 and C_7F_{14} will be discussed.

As expected, electron capture by SF_6 and C_7F_{14} at atmospheric pressure occurs primarily by the resonance EC process leading to molecular anions, M^-. However, for both of these compounds, minor fragment ions of the type $(M-F)^-$ are observed in about 0.10 relative abundance at all temperatures between 30° and 180°C. Figures 10 and 11 show the API mass spectra for SF_6 and C_7F_{14} at 120°C in nitrogen buffer gas, respectively. While a portion of these $(M-F)^-$ ions are known to be produced along with the M^- species in a branched EC reaction (50), most of the $(M-F)^-$ ions are formed in an atmospheric pressure buffer gas by the reaction of the M^- species with trace water vapor (51). In view of these side reactions, the largest possible molecular regeneration coefficient, χ, that might have been expected for either SF_6 or C_7F_{14} is about 0.90, rather than 1.00, even if reaction 2 proceeds entirely by pathway 2a. Therefore, the observation that $\chi \approx 0.80$ for C_7F_{14} at all temperatures actually suggests that about 90% of the molecular anions of this compound are converted back to the parent molecule upon recombination by pathway 2a. While the χ values reported for SF_6 in Table 2

will be similarly increased by about 10% by correction for this effect, this correction is of little significance for the case of SF_6, where destruction is clearly dominated by the IIR reaction (for example, χ = 0.13 at 30°C is increased only to about χ = 0.14 by this correction).

Figures 12 through 15 show the API mass spectra of C_6F_{12} at 30°, 75°, 120°, and 180°C in nitrogen buffer gas. Like SF_6 and C_7F_{14}, the EC reaction proceeds primarily by the resonance process. However, the fragment ion $(M-F)^-$ is in greater relative abundance for C_6F_{12} than for SF_6 and C_7F_{14}, and its abundance varies with temperature. The absolute intensities of the $(M-F)^-$ ions are 0.28, 0.31, 0.33, and 0.40 at 30°, 75°, 120°, and 180°C respectively. Although a portion of the $(M-F)^-$ ions of C_6F_{12} are undoubtly formed by the reaction of M^- with trace water vapor, the temperature dependance of the formation of the $(M-F)^-$ ion is most likely explained by a branched EC reaction of the type shown in Reaction 28.

$$M + e \rightleftharpoons (M^-)^* \begin{cases} \nearrow M^- & (28a) \\ \searrow (M-F)^- & (28b) \end{cases}$$

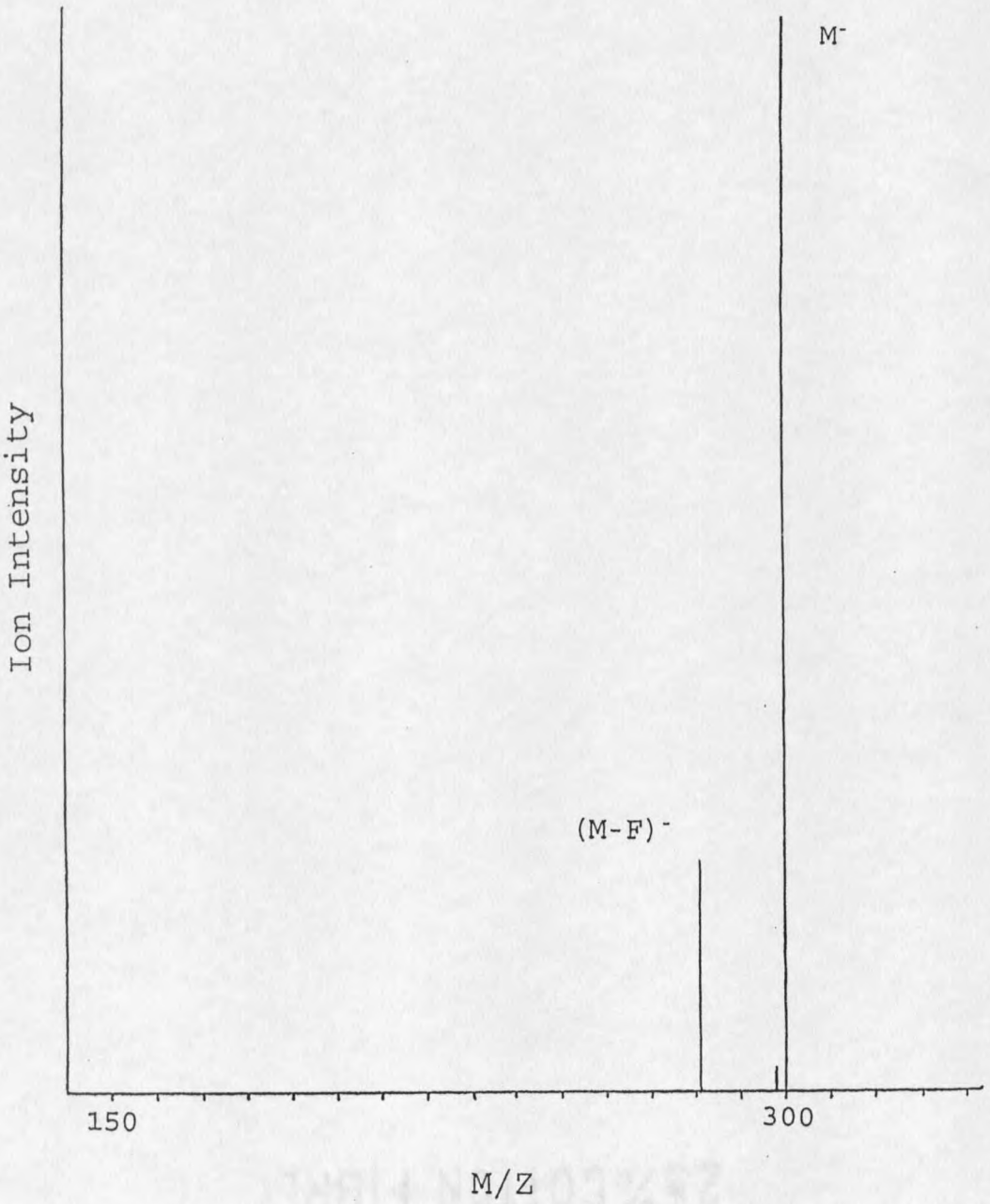

Figure 12. API mass spectrum of C_6F_{12} at 30°C in nitrogen buffer gas.

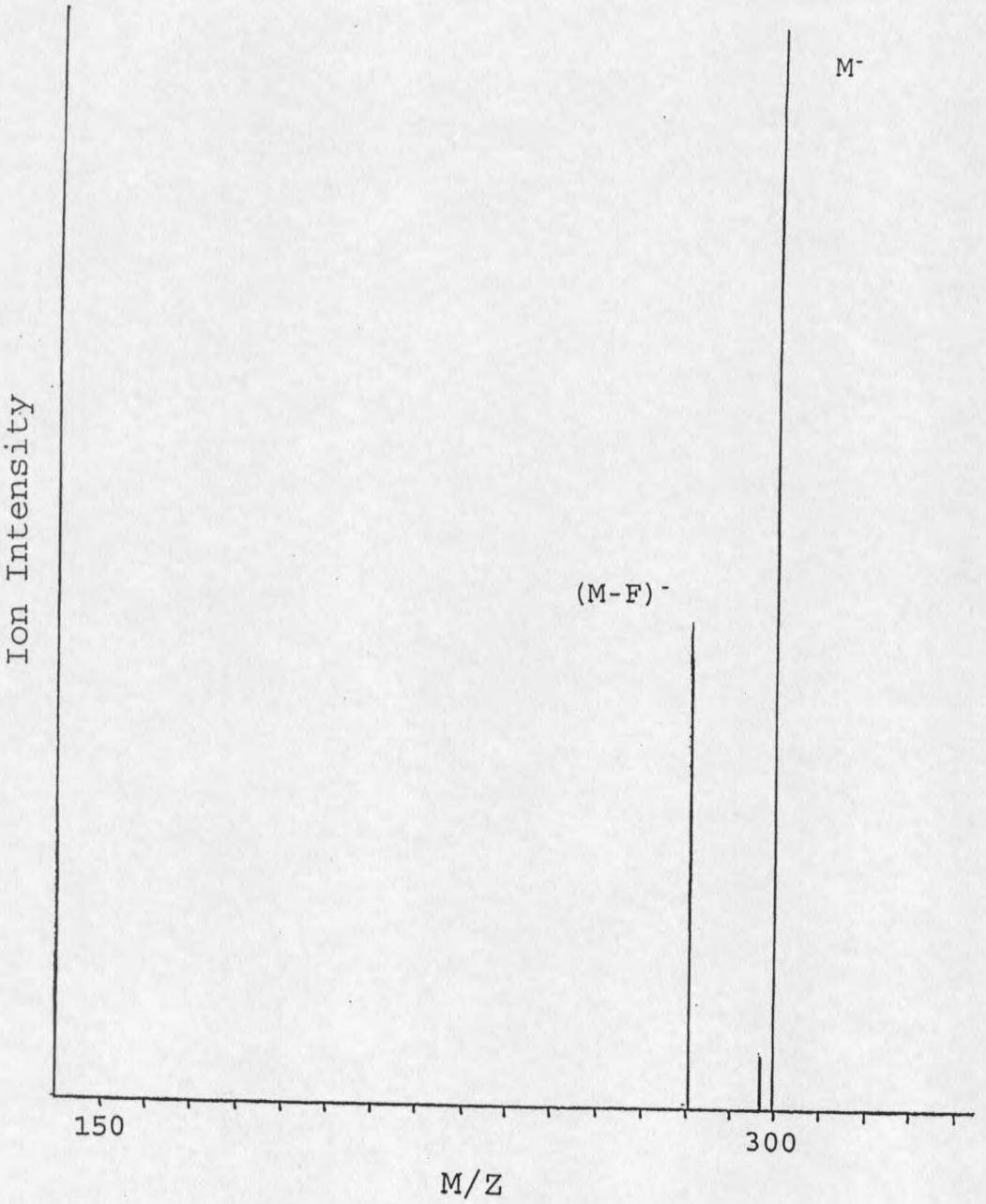

Figure 13. API mass spectrum of C_6F_{12} at 75°C in nitrogen buffer gas.

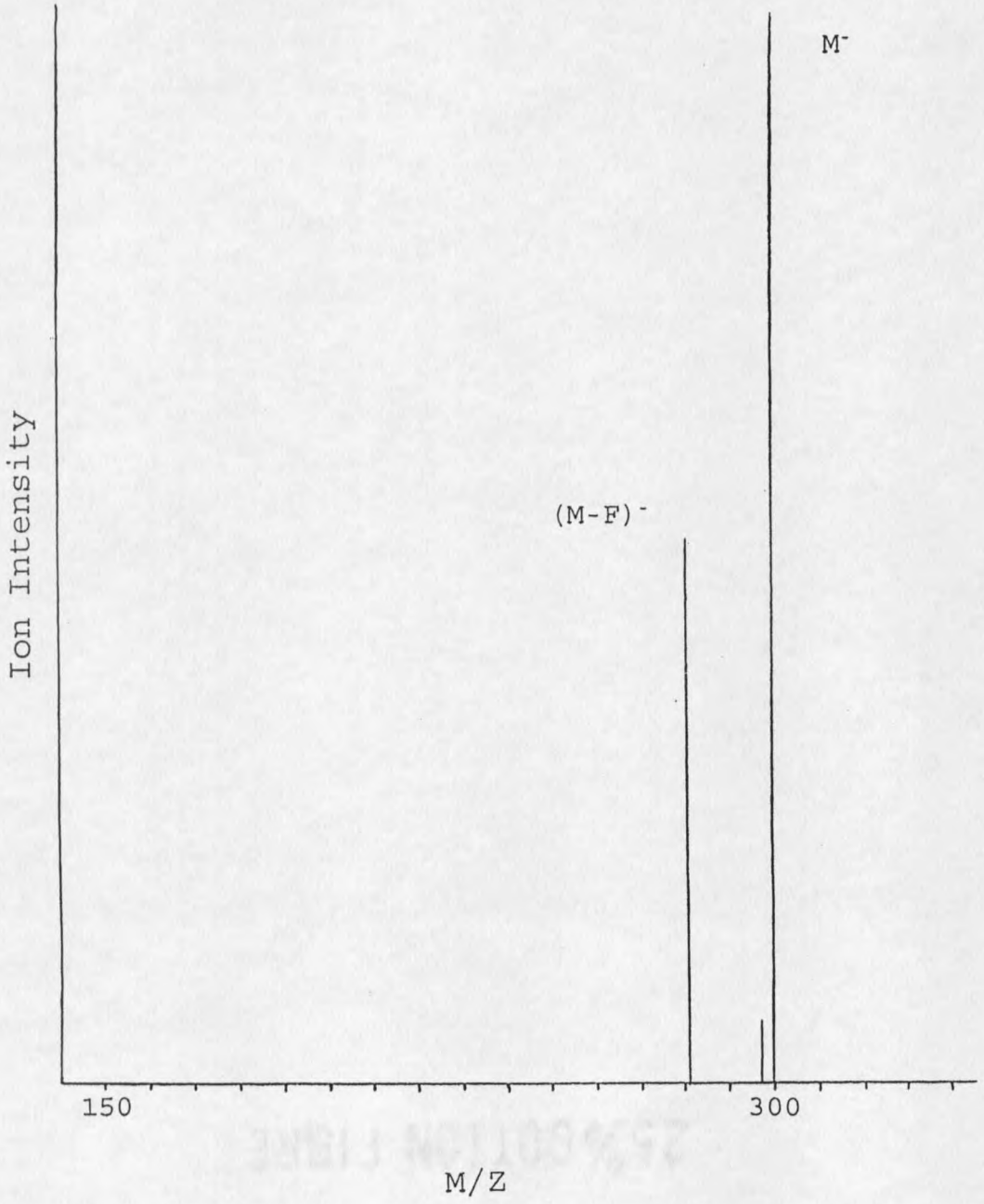

Figure 14. API mass spectrum of C_6F_{12} at 120°C in nitrogen buffer gas.

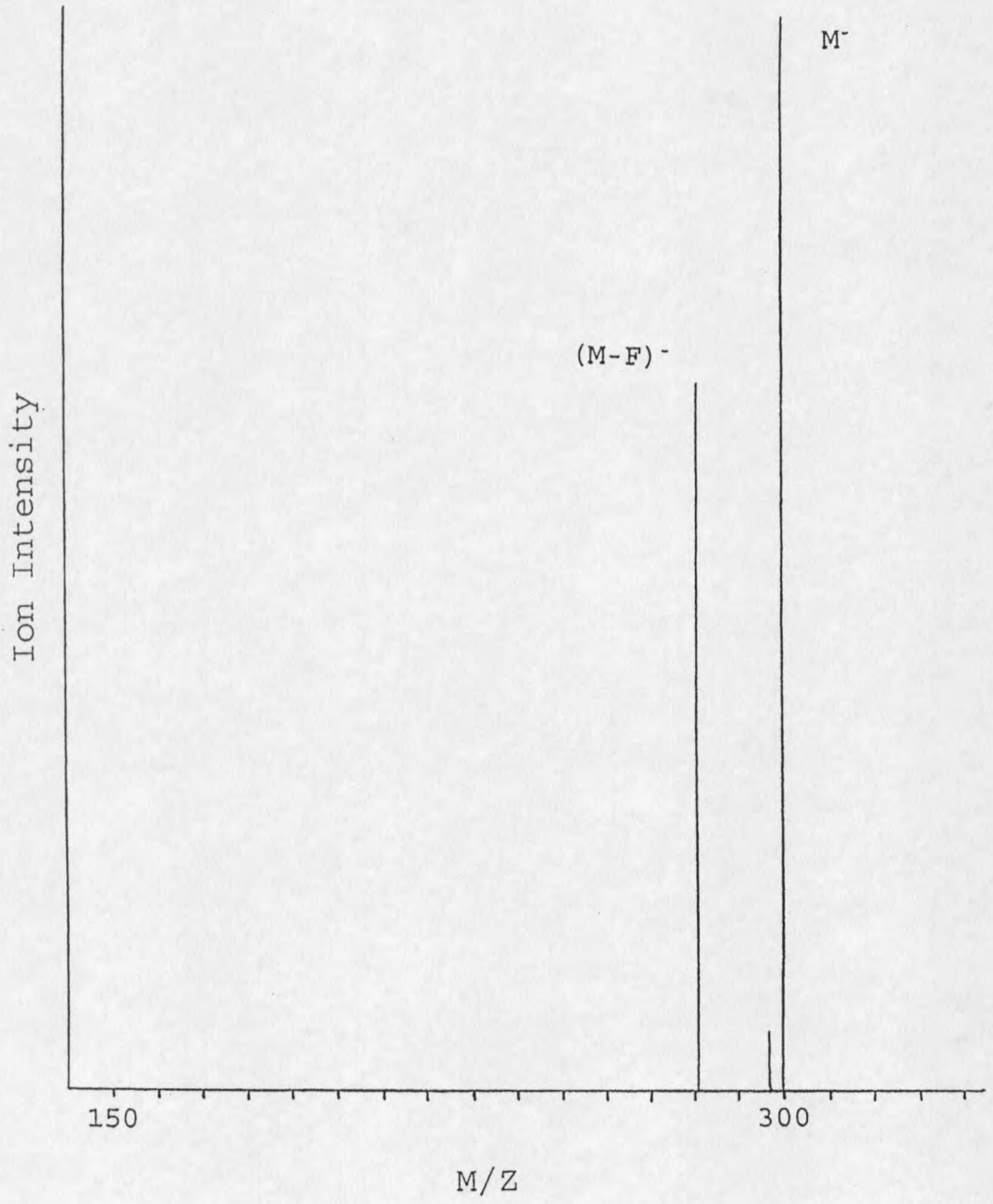

Figure 15. API mass spectrum of C_6F_{12} at 180°C in nitrogen buffer gas.

The excited intermediate, $(M^-)^*$, initially formed upon EC, is quenched by collisions with buffer gas molecules to form M^- (reaction 28a). Alternatively, $(M^-)^*$ may decay to form $(M-F)^-$ (reaction 28b). The rate constant for the decay reaction, 28b, has been shown to increase with increasing temperature for other perfluoro compounds (50). Therefore, it is reasonable to predict that C_6F_{12} might behave in a similar manner and that the intensity of the $(M-F)^-$ would increase due to the increased rate of reaction 28b relative to that of reaction 28a with increasing temperature.

Considering the API mass spectra for C_6F_{12}, the maximum χ value for this compound are 0.72, 0.69, 0.67, and 0.60 at 30°, 75°, 120°, and 180°C respectively. The experimentally determined χ values of 0.71, 0.67, 0.63, and 0.56 listed in Table 2 for C_6F_{12} at the above temperatures demonstrate that at least 93% of the parent molecule is regenerated upon IIR.

Effect of Positive Ions on IIR Fate of SF_6^- and $C_7F_{14}^-$.

The positive ions in the API background mass spectrum shown in Figure 8 are thought to be the same ions normally present in the reactor cell, along with an assortment of ions originating from unavoidable "column bleed" molecules introduced from

column #1 in Figure 2. For SF_6 and C_7F_{14}, experiments were performed in which this uncontrolled set of positive ions was converted to a more controlled set by the addition of trimethylamine (TMA) to the carrier gas. TMA undergoes reactions similar to those of triethlyamine shown in reactions 21a-c to produce $(TMA+H)^+$ and $(TMA-H)^+$ and also the proton clusters $H^+(TMA)_{1-2}$ (44). Table 3 shows the results of these experiments. When compared to the results in Table 2, the addition of TMA to the carrier gas has essentially no effects on the α and χ values observed for these two compounds.

Table 3.

Values of α and χ at 180°C with the addition of trimethylamine to the carrier gas[a].

Compound	α (cm^3 sec^{-1})	χ
SF_6	3.7×10^{-7}	0.17
C_7F_{14}	3.4×10^{-8}	0.74

[a] Electron densities, β, and uncertainties are the same as listed in Table 2.

Two potential effects of adding TMA to the carrier gas have been considered. First, is that all possibility of positive ion-molecule reactions where the neutral is SF_6 or C_7F_{14} would be shut off by the formation of the very stable TMA

derived positive ions. Since no effects of TMA were observed, it is concluded that positive ion-molecule reactions are not of importance in the reaction cell. This result is not surprising since the rate constants for even fast ion-molecule reactions are much slower than the EC rate constants for SF_6 and C_7F_{14}. Furthermore, Morris et al. (15) have recently shown that even more energetic ions, such as NO^+ and $H^+(H_2O)$ are unreactive towards small perfluoro compounds.

The addition of TMA to the carrier gas is expected to have a large effect on the overall exothermicity of the IIR reactions. For example, by addition of TMA, some of the positive ions would be converted from $H^+(H_2O)$ to $H^+(TMA)$. By this change, the exothermicity of all IIR reactions involving these two ions would be very significantly reduced, by about 60 kcal mol^{-1} assuming the proton affinities of H_2O and TMA are 165 and 225 kcal mol^{-1} respectively (52). One of the least exothermic reactions envisioned to occur would be that of the $H^+(TMA)_2$ ion with the $C_7F_{14}^-$ ion, for which the most likely products can now be stated to be the C_7F_{14} molecule, the H atom, and two TMA molecules. The heat of this reaction is still expected to be exothermic by 43 kcal mol^{-1}, assuming an H atom ionization energy of 313 kcal mol^{-1} (53), an electron

affinity for C_7F_{14} of 23 kcal mol^{-1} (54), and a heat of TMA clustering to $H^+(TMA)$ of -22 kcal mol^{-1} (55). Since no detectable effects of TMA addition were seen, it appears that large changes in the exothermicity of the IIR reactions have little or no effect on the relative importance of molecular regeneration by IIR.

On the Differing IIR Fates of SF_6^-, $C_7F_{14}^-$ and $C_6F_{12}^-$. In considering why the fates of the molecular anions, $C_7F_{14}^-$ and $C_6F_{12}^-$, differ so greatly from that of SF_6^- upon recombination with positive ions, few clues are provided by previous reports of the behavior of these compounds in other negative ion processes. The only known negative ion studies of C_6F_{12} are those of this work and one other (56), in which the EC rate was measured by the swarm technique. A somewhat larger body of work exists for SF_6 and C_7F_{14}. The electron affinities (EA) of SF_6 and C_7F_{14} are almost identical; 1.05 ± 0.10 and 1.06 ± 0.15 eV respectively (54). While they both attach thermal energy electrons very rapidly, neither readily accepts an electron from a donor of lower EA (57). Also, the rates of electron transfer from either SF_6^- or $C_7F_{14}^-$ to a molecule of significantly greater EA have been shown to be unusually slow

(54). The thresholds for electron photodetachment by SF_6^- and $C_7F_{14}^-$ are both unusually high, about 2.2 eV above their EAs (18). These large differences between the EAs and photodetachment thresholds suggest that large structural differences exist between the neutral and negatively ionized forms of both compounds. Another similarity between SF_6^- and $C_7F_{14}^-$ is that both of these anions have been shown to decompose readily in the presence of protic molecules, such as methanol or water (51). In view of these numerous similarities, one might have expected similar behaviors in the IIR reactions of SF_6^- and $C_7F_{14}^-$.

In an attempt to identify the reason for the very different behaviors of SF_6^- and $C_7F_{14}^-$ upon recombination with positive ions, the following areas of speculation have been envisioned. First, if one assumes that the mechanism of the IIR reactions involves the simple transfer of an electron between the approaching counter ions, perhaps the SF_6 neutral species finds itself in a distorted configuration following the electron transfer event from which the stable SF_6 geometry cannot be reattained prior to its dissociation. Support for this suggestion is found in the photodetachment spectra of SF_6^- discussed above (18) and in the fact that the entropy

associated with the negative ionization of SF_6 has been reported to be unusually large (58). With this interpretation, however, one would also have to envision that the corresponding C_7F_{14} neutral species does manage to achieve its stable configuration after electron transfer, in spite of similar photodetachment evidence (18) for large geometric differences between its neutral and negatively ionized forms. Additional points of speculation come to mind if recombination events can also occur by the transfer of ions, such as F^-, rather than just by an electron, between more closely interacting counterions. If so, perhaps SF_6^- recombines in this manner, while $C_7F_{14}^-$ does not. Alternatively, if the counterions physically combine to form a reaction complex, as is commonly thought to occur in ion-molecule reactions, differing behaviors of SF_6^- and $C_7F_{14}^-$ within these reaction complexes might occur. Because so little is known concerning the detailed mechanisms of IIR reactions, it is presently difficult to assess the relative merits of these possibilities.

Implications for the Atmospheric Chemistry of SF_6, C_7F_{14}, and C_6F_{12}. If it is momentarily assumed that the present results directly apply to the physical conditions existing in the earth's mesosphere, the following predictions can be made. Atmospheric SF_6 will be destroyed in the mesosphere by its sequential EC/IIR reactions, while C_7F_{14} and C_6F_{12} will not be destroyed by their EC/IIR reactions. However, since the pressure in the mesosphere is at least three orders of magnitude lower than the pressure used in this work, the following expected effects should also be considered. The basic mechanism of IIR reactions at pressures existing in the mesosphere is bimolecular, while the mechanism is termolecular in the atmospheric pressure range due to energy absorbing collisions of buffer gas molecules with at least one of the interacting counterions. Therefore, in the high pressure experiments of this work, a portion of the exothermicity of the IIR reactions is imparted to the buffer gas molecules, rather than to the ions alone, as in the bimolecular mechanism of the mesosphere. In addition, a large portion of the positive ions existing in the mesosphere, such as O_2^+ and NO^+ (59), will be of higher energy than those utilized for the present study. This change would impart greater energies to

the counterions at the instant of recombination. Both of the factors just mentioned might cause greater destruction of the counterions at low pressures, in spite of the evidence provided from the present work that the fates of the negative ions were not noticeably affected by large changes in the reaction exothermicity. In that case, the destruction of SF_6 in the mesosphere by EC/IIR reactions would still be assured, while the degree of C_7F_{14} and C_6F_{12} destruction by their EC/IIR reactions in the mesosphere might be greater than predicted on the basis of the present measurements.

χ Values for Nitronbenzene and Several Substituted Nitrobenzenes

The regeneration coefficient results for the nitrobenzenes studied are summarized in Table 4. These particular nitro-

Table 4.

Summary of results for nitrobenzenes at 120°C.

Compound	electron density[a]	β (cm^3 sec^{-1})[b]	H_1/H_2	α (cm^3 sec^{-1})	χ
NB	$8.2x10^7$	$2.6x10^{-8}$	1.35	$1.2x10^{-9}$	0.95±0.01
o-NO_2NB	$6.5x10^7$	$1.3x10^{-7}$	16.1	$5.3x10^{-8}$	0.59±0.12
m-NO_2NB	$7.0x10^7$	$2.2x10^{-8}$	1.66	$2.4x10^{-9}$	0.89±0.03
p-NO_2NB	$7.0x10^7$	$1.4x10^{-7}$	25.0	$8.9x10^{-8}$	0.37±0.18
p-FNB	$3.7x10^7$	$3.5x10^{-8}$	1.41	$5.7x10^{-9}$	0.84±0.05

Table 4. (continued)

[a] Electron density was determined using $CHCl_3$ as the reference compound.

[b] β was obtained from reference 46 as determined by the PHPMS method at 125°C in 10 Torr methane buffer gas.

benzenes were chosen because their resonance EC rate constants have been previously determined (60), and due to their compatibility with the chromatography set-up associated with the reaction/dummy cell apparatus.

The χ values range from a high of 0.95 for nitrobenzene, NB, to a low of 0.37 for para dinitrobenzene, p-NO_2NB. These results are interesting in that no obvious trend is apparent in the amount of compound regenerated upon IIR. For example, the electron affinities of o-NO_2NB and m-NO_2NB are both 1.65 eV (61), implying equal exothermicities for their IIR reactions, however, their χ values differ substantially. On the other hand, the EAs of NB and p-FNB (para fluoronitrobenzene) are close (1.01 and 1.12 eV respectively (61)) and both exhibit similarly large χ value. The compound with the largest EA, P-NO_2NB, exhibits the least amount of regeneration upon recombination. Many of the nitrobenzenes are reported to have negative entropies of negative ionization,

ΔS_a° (61). Two of the compounds studied here, NB and p-NO_2NB, have reported ΔS_a° values of -1.0 and -4.5 cal/K respectively (61). When these values are compared with that of SF_6 (ΔS_a° = +18 cal/K), it is clear that large structural differences in the molecular anions, resulting from EC, do not necessarily have an effect on the subsequent IIR reactions. As in the case of the perfluoro compounds discussed in the previous sections, it is difficult to completely assess the results obtained for the IIR reactions of these nitrobenzenes.

EC Rate Constants for Dissociatively Attaching Compounds

The reaction/dummy cell apparatus was used to determine EC rate constants for compounds that attach electrons by the dissociative mechanism. For these compounds, χ is assumed to equal zero, thereby allowing the experimentally determined value, α, to be a direct measure of the EC rate constant for the compound of interest (Equation 25). The results of these studies are summarized in Table 5.

Table 5.

EC rate constants for dissociatively attaching compounds as determined by the reaction/dummy cell apparatus.

Compound	Temp (°C)	Electron density	H_1/H_2	α (cm^3sec^{-1}) [a]	β (cm^3sec^{-1}) [b]
1,2 dibromo-tetraflouroethane	30	$8.4x10^6$	7.6	$2.7x10^{-7}$	$1.6x10^{-7}$ [g] (25°C)
	75	$6.4x10^6$	5.6	$2.4x10^{-7}$	
	120	$4.0x10^6$	5.0	$3.4x10^{-7}$	$2.4x10^{-7}$ (107°C)
	180	$2.4x10^6$	3.4	$3.4x10^{-7}$	$3.0x10^{-7}$ (202°C)
1,2 dibromo-1,1 difluoroethane	30	$8.4x10^6$	6.5	$2.2x10^{-7}$	
	75	$6.4x10^6$	5.0	$2.1x10^{-7}$	
	120	$4.0x10^6$	4.7	$3.1x10^{-7}$	$2.0x10^{-7}$ [c]
	180	$2.4x10^6$	3.1	$3.0x10^{-7}$	
$CHFBr_2$	30	$8.4x10^6$	4.0	$1.2x10^{-7}$	
	75	$6.4x10^6$	3.3	$1.2x10^{-7}$	
	120	$4.0x10^6$	2.6	$1.4x10^{-7}$	$1.5x10^{-7}$ [c]
	180	$2.4x10^6$	2.4	$1.9x10^{-7}$	
1,2 dibromo-1,1,2 trifluoroethane	30	$8.4x10^6$	6.3	$2.1x10^{-7}$	
	75	$6.4x10^6$	5.0	$2.1x10^{-7}$	
	120	$4.0x10^6$	4.1	$2.6x10^{-7}$	$2.2x10^{-7}$ [c]
	180	$2.4x10^6$	2.9	$2.6x10^{-7}$	
CCl_3Br	30	$1.2x10^7$	5.6	$1.3x10^{-7}$	$8.2x10^{-8}$ [d]
	75	$7.9x10^6$	7.8	$2.9x10^{-7}$	
	120	$6.5x10^6$	7.6	$3.5x10^{-7}$	$1.1x10^{-7}$ [c]
	180	$4.0x10^6$	6.1	$4.3x10^{-7}$	

Compound	Temp (°C)	Electron density	H_1/H_2	α (cm^3sec^{-1}) [a]	β (cm^3sec^{-1}) [b]
CH_2Br_2	30	$8.4x10^6$	3.1	$8.4x10^{-8}$	$9.4x10^{-8}$ [e]
	75	$6.4x10^6$	2.6	$8.6x10^{-8}$	$1.2x10^{-7}$
	120	$4.0x10^6$	2.6	$1.3x10^{-7}$	$1.4x10^{-7}$
	180	$2.4x10^6$	2.1	$1.6x10^{-7}$	$1.6x10^{-7}$
CH_3I	30	$8.4x10^6$	4.6	$1.4x10^{-7}$	
	75	$7.2x10^6$	3.9	$1.4x10^{-7}$	
	120	$5.6x10^6$	3.4	$1.4x10^{-7}$	$1.4x10^{-7}$ [c]
	180	$3.2x10^6$	2.7	$1.8x10^{-7}$	$1.8x10^{-7}$ [e]
CCl_4	30	$1.0x10^7$	22.7	$7.4x10^{-7}$	$3.9x10^{-7}$ [f]
	75	$7.3x10^6$	18.5	$8.2x10^{-7}$	$3.8x10^{-7}$
	120	$5.8x10^6$	13.7	$7.4x10^{-7}$	$3.8x10^{-7}$
	180	$3.2x10^6$	7.4	$6.8x10^{-7}$	$3.7x10^{-7}$
1,2 dibromo-hexafluoropropane	30	$8.4x10^6$	20.8	$8.0x10^{-7}$	
	75	$7.2x10^6$	14.5	$6.4x10^{-7}$	
	120	$5.6x10^6$	10.6	$5.9x10^{-7}$	$4.2x10^{-7}$ [c]
	180	$3.2x10^6$	5.8	$5.0x10^{-7}$	
$CHBr_3$	30	$8.5x10^6$	4.6	$1.4x10^{-7}$	
	75	$5.1x10^6$	2.6	$1.1x10^{-7}$	
	120	$5.0x10^6$	2.3	$8.8x10^{-8}$	$1.3x10^{-7}$ [c]
	180	$3.4x10^6$	1.6	$6.1x10^{-8}$	
1,1,2,2 tetrachloroethane	30	$1.6x10^7$	4.5	$7.4x10^{-8}$	
	75	$5.1x10^6$	1.46	$3.1x10^{-8}$	
	120	$5.0x10^6$	1.29	$2.0x10^{-8}$	$5.1x10^{-8}$ [c]
	180	$3.4x10^6$	1.33	$3.3x10^{-8}$	

[a] α is the experimentally determined EC rate constant. The uncertainty is about 25%.

Table 5. (continued)

[b] β is the EC rate constant from the literature (0.5 Torr helium buffer gas), or from dual cell ECD experiments of this work.

[c] As determined by the dual cell ECD method from this work.

[d] From reference (62)

[e] From reference (17)

[f] From reference (16)

[g] From reference (49)

The experimentally determined EC rate constants listed in Table 5 are in rather good agreement with previous results from the FALP method (16,17,49,62) or the dual cell ECD method used in the present work. Two major exceptions are noted however. The EC rate constants determined for CCl_4 and 1,2 dibromohexafluoropropane, $C_3Br_2F_6$, are substantially greater than the results obtained from different methods (FALP for CCl_4 (17) and dual ECD for $C_3Br_2F_6$), and also exceed the theoretical maximum value (63) for an EC reaction of about 5.0×10^{-7} cm^3 sec^{-1} by as much as 64%. These results infer that a greater amount of the compound is being destroyed in the reaction cell than what would have been expected from the EC reaction alone. Three possible explanations for the excess

loss of these two compounds within the reaction cell can be envisioned. The first is an ion-molecule reaction where the neutral is CCl_4 or $C_3Br_2F_6$. However, the ion-molecule reaction is not expected to compete with the much faster EC reaction. In order to positively rule out this possibility, TMA was added to the carrier gas to create a very stable, unreactive set of positive ions, and the experiment with CCl_4 was then repeated at 180°C. As expected, addition of TMA to the carrier gas had essentially no effect on the determined EC rate constant (an increase of only 3% was observed relative to the case in which no TMA was present). Therefore, ion-molecule reactions can be ruled out as the cause of the excess destruction of CCl_4 and $C_3Br_2F_6$ occurring within the reaction cell.

The second possible explanation for the excess destruction of CCl_4 and $C_3Br_2F_6$ is the reaction of these compounds with gas phase radicals that originate from trace buffer gas impurities. However, the rate constants for the fastest radical-neutral reactions have rate constants that are on the order of 1×10^{-10} cm^3 sec^{-1} (26), approximately three orders of magnitude less than the EC reactions of CCl_4 and $C_3Br_2F_6$. Therefore, unless the density of gas phase radicals is

more than three orders of magnitude greater than that of electrons, it is not anticipated that radial-neutral reactions can compete effectively with EC for the destruction of these compounds.

The final explanation envisioned for the excess loss of these compounds is a surface-assisted destruction mechanism occurring on the walls of the reaction cell. Previous reports by Sears et al. (26) and Culbertson et al. (64) have demonstrated that surface assisted reactions can be very efficient and the products of these reactions can dominate the high pressure electron capture (HPEC) mass spectrum obtained at 0.1 Torr buffer gas pressure. In those studies, it was shown that neutral analyte molecules could diffuse to the walls of the ion source where they were altered by reactions with radical species, such as $H\cdot$ and $CH_3\cdot$, that were present on the surface. One significant difference between these studies and the present work, however, is the buffer gas pressure. Diffusion of neutral molecules at 1010 Torr (present conditions) will be much slower than the HPEC conditions (0.1 Torr). It is therefore necessary to calculate the first order rate constant for diffusion at 1010 Torr and compare it with the main competitive process, EC, to determine if a surface

assisted destruction mechanism is feasible.

The first order rate constant for diffusion is again given by $D_n\Lambda^{-2}$, where D_n is the diffusion coefficient of the neutral and Λ is the characteristic diffusion length of the reaction cell (25). The magnitude of D_n can be calculated using Equation 29,

$$D_n = \frac{\sqrt{v_1^2 + v_2^2}}{3\pi n \delta_{12}^2} \qquad (29)$$

where v_1 and v_2 are the most probable velocities of the neutral of interest and the buffer gas, n is the buffer gas density, and δ_{12} is the average molecular diameter of the neutral and buffer gas molecule. Using δ_{12} equals 6 x 10^{-8} cm for all neutrals (26) and v equals 5.2 x 10^4 cm sec^{-1} and 2.2 x 10^4 cm sec^{-1} for N_2 and CCl_4 respectively, D_n for CCl_4 is then 0.12 cm^2 sec^{-1}. A value of Λ may be obtained by dividing the radius of the reaction cell(0.4 cm) by π. Therefore, Λ = 0.13 cm and the first order rate constant of diffusion for CCl_4 at 180°C is then 7.1 sec^{-1}. Comparing this to the pseudo first order EC rate constant for CCl_4 of 1.8 sec^{-1}, (obtained from $k_{obs} = k_{EC}[e]$, where k_{ec} = 3.7 x 10^{-7} cm^3 sec^{-1} (16) and [e] = 4.8 x 10^6 cm^{-3}), it is reasonable to predict that the surface-assisted destruction of CCl_4 and $C_3Br_2F_6$ could be operative under the

present conditions of 1010 Torr based on the fact that the rate constant for diffusion is about four times greater than that of electron capture. Upon contact with the surface of the reaction cell wall, CCl_4 and $C_3Br_2F_6$ could be altered by reactions with radical species or some other surface contaminant. This would then account for the excess loss of these compounds with the reaction cell.

The reaction/dummy cell apparatus has proven to be an effective way of determining EC rate constants for dissociatively attaching compounds. For compounds whose determined EC rate constants are suspected of being too large, the dual cell ECD experiment provides an excellent check of the reaction/dummy cell method, since no evidence of the side reactions or inflated EC rate constants discussed above has been observed with the dual ECDs.

SUMMARY

Gas phase ion-ion recombination can provide the dominant loss mechanism for ions within partially ionized gases under many commonly encountered physical conditions. For this reason, many studies have investigated the rates of IIR reactions, and many theories have been devised to explain the mechanism by which IIR occurs. However, very little is known about the neutral products formed from IIR reactions, in spite of the importance that these products can have on atmospheric chemistry and to the response of certain analytical detectors. The results from one previous study that investigated the products of IIR using a dual cell ECD were based on two critical assumptions that could not be proven experimentally. Therefore, the focus of this work has been to build an apparatus to definitively study the products of IIR reactions at atmospheric pressure. More specifically, this apparatus was used to determine the extent to which molecular anions were regenerated to their parent neutral upon recombination with positive ions. This apparatus was also used to determine EC rate constants for dissociatively electron attaching

compounds. In addition, experiments using an atmospheric pressure ionization mass spectrometer were performed to determine what effect the nature of the recombining ions had on the rate of IIR.

When two polyatomic ions of opposite charge undergo recombination, the neutral products can be fragments of the recombining ions, or if a simple electron transfer mechanism is operative, the parent molecules can be regenerated. If an electron attaching compound undergoes resonance electron capture to form its molecular anion and the parent neutral is regenerated upon IIR, it may then undergo a second EC/IIR reaction. This process could occur many times while the compound is within the ECD. Hence, the ECD response to this compound would be enhanced relative to the case in which the parent molecule is not regenerated upon IIR. The regeneration mechanism could also have a very important effect on the atmospheric chemistry of perfluoro compounds. Many perfluoro compounds, such as SF_6, attach electrons very rapidly and are also extremely immune to the oxidative and photochemical processes that destroy most compounds in the troposphere or stratosphere. Therefore, such compounds can enter the mesosphere where reactions with free electrons may occur. If

the compound is then regenerated upon the subsequent IIR reaction, it could significantly increase its atmospheric lifetime, which is important because most PFCs are efficient greenhouse gases.

Three PFCs, SF_6, C_7F_{14}, and C_6F_{12}, all of which undergo resonance EC, were studied using the reaction/dummy cell apparatus to determine the extent to which the molecular anion was regenerated upon IIR. By comparing the ECD response to the compound of interest surviving passage through the reaction cell (where EC and IIR occur), to that of the dummy cell, (where no reactions take place), in conjunction with the conservation equations that describe the cell, conclusions were drawn about the amount of compound being regenerated upon IIR. The results showed that the molecular anions of C_7F_{14} and C_6F_{12} are almost completely regenerated to their parent neutral upon IIR, while recombination of the molecular anion of SF_6 with positive ions tends to form other unknown neutral species. In order to draw these conclusions based on the experimental data obtained from the reaction/dummy cell apparatus, it was also necessary to know the EC rate constant for these compounds at atmospheric pressure. This was achieved by using a dual cell ECD in the following manner. A gaseous

sample containing the compound of interest and the dissociatively electron attaching reference compound, $CFCl_3$, were chromatographically introduced to the dual cell ECD. Instrumental parameters could be varied on the dual cell ECD such that regeneration of the compound of interest upon IIR could be reduced to a negligible level. Under these conditions, the molar ECD response of these compounds will reflect their relative EC rate constants. Because the EC rate constant of $CFCl_3$ is well known, the relative EC rate constant for the compound of interest could be determined.

For compounds that capture electrons by the dissociative mechanism, the reaction/dummy cell apparatus was found to be very useful for the determination of EC rate constants. Since regeneration of the parent molecule from IIR is not possible for these compounds, the experimentally determined quantity was directly equal to the EC rate constant. The results obtained by this method were in good agreement with previous measurements, when available. For those compounds whose EC rate constants had not been previously measured, the dual cell ECD was used in the manner described above as a second determination of the EC rate constant. The results between the these two methods were also in good agreement. Two exceptions

to the good agreement between methods were noted. For CCl_4 and 1,2 dibromohexafluoropropane ($C_3Br_2F_6$), the EC rate constants determined by the reaction/dummy cell method were substantially greater than those of the other methods, and also exceeded the maximum value predicted by theory by as much as 64%. Some process was destroying more of these compounds in the reaction cell than what was expected. A possible explanation for the excess loss of these compounds in the reaction cell is thought to be a surface assisted destruction mechanism. It is considered feasible for the neutral CCl_4 or $C_3Br_2F_6$ molecule to diffuse to the surface of the reaction cell where it could react with radical species or other impurities present on the surface to form an altered compound, thereby accounting for the additional destruction of these compounds.

To determine what effect the nature of the recombining ions has on the rate of IIR, an experiment was devised using the APIMS as follows. First, a stable set of positive ions was created in the APIMS ion source by the addition of triethylamine to the buffer gas. Second, strongly electron attaching compounds were introduced to the ion source to saturate the negative charge side of the plasma. Compounds were chosen such that Cl^-, Br^-, I^-, SF_6^-, and $C_7F_{14}^-$ were

produced upon EC. The total positive ion signal was then monitored while the electron attaching compounds were introduced. The intensity of the total positive ion signal is proportional to $(1/R)^{1/2}$, where R is the recombination rate constant. Thus, by comparing the change in the positive ion signal when the EC active compound enters the ion source, the relative IIR rate constants could be determined. The first observation of this experiment was that the positive ion signal increased when the EC active compounds were introduced. This infers that positive ion-electron recombination is faster than ion-ion recombination. This result was expected based on literature values for the rate constants for these two reactions. The second observation was that the positive ion signal increased by the same amount, irrespective of the nature of the negative ion. This indicates that the nature of the ions used for this study had no effect on the IIR rate constant. The rate constant for IIR, based on the percent increase of the positive ion signal, was calculated to be 2.0 x 10^{-6} cm^3 sec^{-1}, which is in excellent agreement with the literature values.

LITERATURE CITED

1. Bowers, M. T.; Gas Phase Ion Chemistry, Vol I, Acedemic Press: New York, 1979.

2. Bowers, M. T.; Gas Phase Ion Chemistry, Vol II, Acedemic Press: New York, 1979.

3. Bowers, M. T.; Gas Phase Ion Chemistry, Vol III, Acedemic Press: New York, 1984.

4. Watson, J. T.; Introduction to Mass Spectrometry, Raven Press: New York, 1985.

5. Harrison, A. G. Chemical Ionization Mass Spectrometry, Second Edition, CRC Press: Boca Raton, 1992?

6. Zlatkis, A.; Poole, C. F.; Electron Capture, Theory and Practice in Chromatography, Elsevier: New York, 1981.

7. Carroll, D. I.; Dzidic, I.; Horning, E. C.; Stillwell, R. N. Appl Spectros Rev. **1981, 17,** 337.

8. Eiceman, G. A.; Karpas, Z.; Ion Mobility Spectrometry, CRC press: Boca Raton, 1994.

9. Fenn, J. B.; Mann, M.; Meng, C. K.; Wong, S. F.; Whitehouse, C.; Science. **1989, 246,** 64.

10. Adams, N. G.; Smith, D.; in Techniques for the Study of Ion Molecule Reactions, John Wiley and Sons: New York, 1988.

11. Kebarle; P.; in Techniques for the Study of Ion Molecule Reactions, John Wiley and Sons: New York, 1988.

12. Lovelock, J. E.; Lipsky, S. R.; J Am Chem Soc. **1960, 82,** 431.

13. Siegel, M. W.; McGowen, M. C.; J Chromatogr. **1976, 122,** 397.

14. Grimsrud, E.P.; Warden, S. W.; Anal Chem. **1980, 52,** 1842.

15. Morris, R. A.; Miller, T. M.; Viggiano, A. A.; Paulson, J. F.; Solomon, S.; Reid, G.; J Geophys Res. **1995, 100,** 1287.

16. Smith, D.; Adams, N. G.; Alge, E.; J Phys B: At Mol Phys. **1984, 17,** 461.

17. Alge, E.; Adams, N. G.; Smith, D.; J Phys B: At Mol Phys. **1984, 17,** 3827.

18. Mock, R. S.; Grimsrud, E. P.; Chem Phys Lett. **1991, 184,** 99.

19. Barrow, G. M.; Physical Chemistry, McGraw Hill: New York, 1979, 4th ed.; chapter 2.

20. Meot-Ner, M.; in Gas Phase Ion Chemistry, Vol I, Bowers, M. T. ed., Acedemic Press: New York, 1979; chapter 6.

21. American Institute of Physics Handbook, 3rd ed.; Marion, J. B.; Gray, D. E., eds., McGraw Hill: New York, 1972; chapter 8, p 184.

22. Gobby, P. L.; Grimsrud, E. P.; Warden, S. W.; Anal Chem. **1980, 52,** 473.

23. Defence Nuclear Agency Reaction Rate Handbook, 4th rev.; Biondi, M. A.; Bortner, M. H.; Baurer, T.; eds.; 1975; chapter 16, pp 16-27.

24. McGowen, S.; Canad J Phys. **1967, 45,** 439.

25. Collision Phenomena in Ionized Gases, McDaniel, E. W.; John Wiley & Sons: New York, 1964; chapter 10.

26. Sears, L. J.; Campbell, J. A.; Grimsrud, E. P.; Biomed and Enviro Mass Spectrom. **1987, 14,** 401.

27. Thomson, J. J.; Rutherford, E. R.; Phil Mag. **1896, 42,** 392.

28. Rutherford, E.; Phil Mag. **1897, 47,** 422.

29. Langevin, P.; Ann Chim Phys. **1903, 28,** 289, 443.

30. Mahan, B. H.; Advances in Chemical Physics, Vol 23; Prigogine, I.; Rice, S. A.; eds.; Wiley: New York, 1973; pp 1-40.

31. Thomson, J. J.; Phil Mag. **1924, 47,** 337.

32. Sayers, J.; Proc Roy Soc (London) Ser A. **1938, 169,** 83.

33. Gardener, M. E.; Phys Rev. **1938, 53,** 75.

34. Machler, W.; Z Physik. **1936, 104,** 1.

35. Mahan, B. H.; Person, J. C.; J Chem Phys. **1964, 40,** 392.

36. Mahan, B. H.; Person, J. C.; J Chem Phys. **1964, 40,** 2851.

37. Natanson, G. L.; Soviet Phys-Tech Phys. **1959, 4,** 1263.

38. Bates, D. R.; Moffett, R. J.; Proc Roy Soc (London) Ser A. **1966, 291,** 1.

39. Bates, D. R.; Flannery, M. R.; Proc Roy Soc (London) Ser A. **1986, 302,** 367.

40. Knighton, W. B.; Grimsrud, E. P.; Anal Chem. **1982, 54,** 1892.

41. Zook, D. R.; Knighton, W. B.; Grimsrud, E. P.; Int J Mass Spectrom Ion Processes. **1991, 63,** 104.

42. Grimsrud, E. P.; Anal Chem. **1978, 50,** 382.

43. Siegel, M. W.; Fite, W. L.; J Phys Chem. **1976, 80,** 2871.

44. Grimsrud, E. P.; J Chromatog. **1984, 312,** 47.

45. Smith, D.; Adams, N. G.; Church, M. J.; J Phys B. **1978, 11,** 4041.

46. Valkenburg, C. A.; Krieger, L. A.; Grimsrud, E. P.; J Chem Phys. **1987, 86,** 6782.

47. Grimsrud, E. P.; Connolly, M. J.; J Chromatogr. **1982, 239,** 397.

48. Peters, D. G.; Hayes, J. M.; Heiftje, G. M.; Chemical Separations and Measurements, Saunders: Philadelphia, 1974.

49. Smith, D.; Herd, C. R.; Adams, N.G.; Paulson J. F.; Int J Mass Spectrom Ion Processes. **1990, 96,** 341.

50. Fehsenfeld, F. C.; J Chem Phys. **1970, 53,** 2000.

51. Knighton, W. B.; Zook, D. R.; Grimsrud, E. P.; J Am Soc Mass Spectrom. **1990, 1,** 372.

52. Szulejko, J. E.; McMahon, T. B.; J Am Chem Soc. **1993, 115,** 7839.

53. Lange's Handbook of Chemistry, Dean, J. A.; McGraw Hill: New York, 1992.

54. Grimsrud, E. P.; Chowdhury, S.; Kebarle, P.; J Chem Phys. **1985, 83,** 1059.

55. Yamdangi, R.; Kebarle, P.; J Am Chem Soc. **1973, 95,** 3504.

56. Pai, R. Y.; Christophorou, L. G.; Christodoulides, A. A.; J Chem Phys. **1979, 70,** 1169.

57. Fehsenfeld, F. C.; J Chem Phys. **1971, 54,** 438.

58. Chowdhury, S.; Heinis, T.; Grimsrud, E.P.; Kebarle, P.; J Phys Chem. **1986, 90,** 2747.